AD-A080 244 AIR FORCE INST OF TECH WRIGHT-PATTERSON AFB OH SCHOO--ETC F/G 20/3
HIGH TEMPERATURE HALL EFFECT IN INDIUM-DOPED SILICON.(U)
DEC 79 6 E RATTRAY
UNCLASSIFIED AFIT/GEP/PH-79D-9 NL

| OF |
AD A
080244

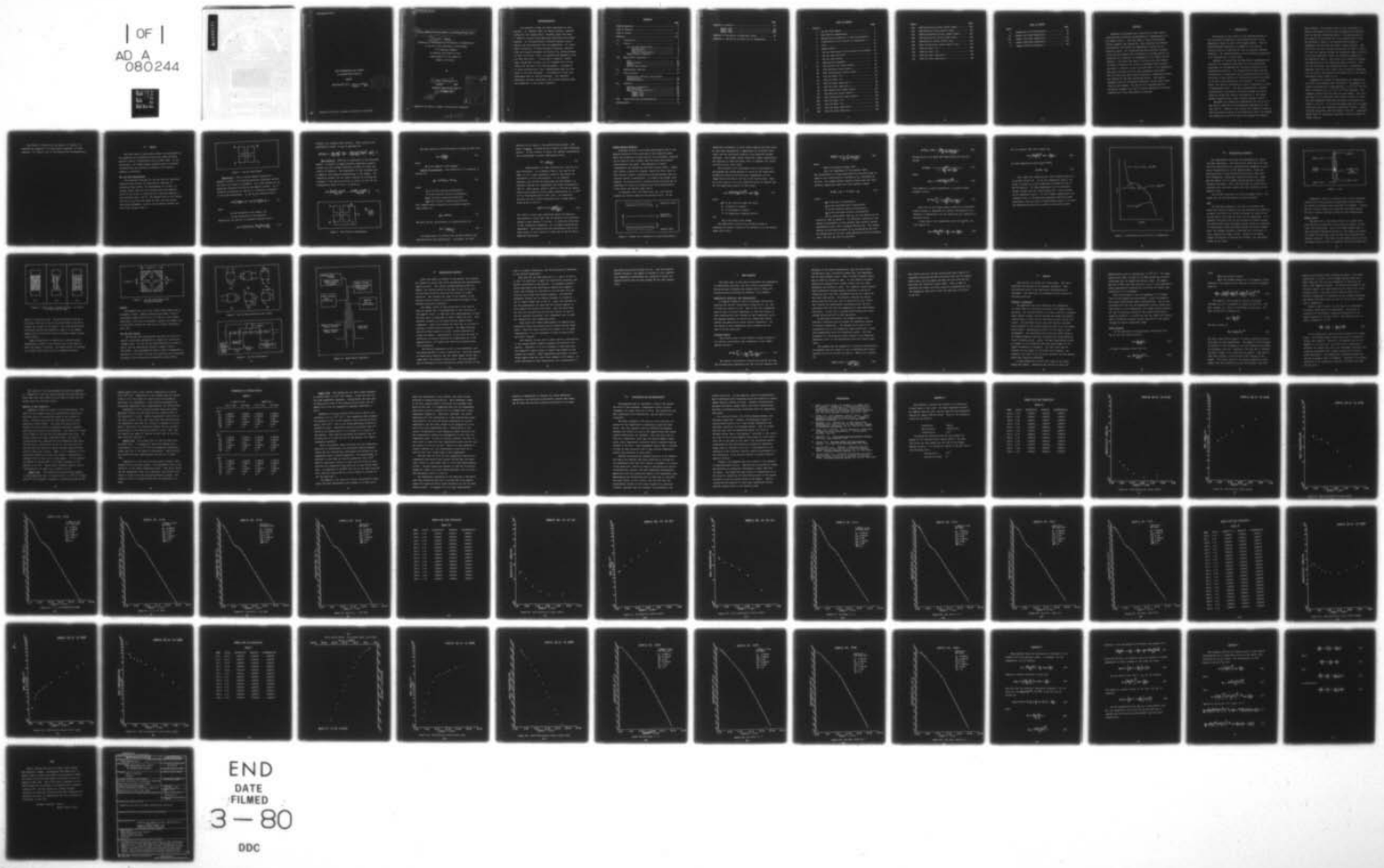

END
DATE
FILMED
3-80
DDC

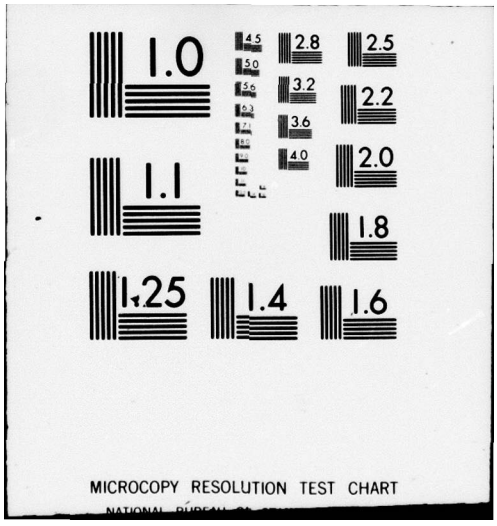
1.0
1.1
1.25
1.4
1.6
1.8
2.0
2.2
2.5
2.8
3.2
3.6
4.0
4.5
5.0
5.6
MICROCOPY RESOLUTION TEST CHART

AFIT/GEP/PH/79D-9

HIGH TEMPERATURE HALL EFFECT IN INDIUM-DOPED SILICON

THESIS

AFIT/GEP/PH/79D-9 Gary E. Rattray
Captain USAF

DDC
RECEIVED
FEB 6 1980
A

Approved for public release; distribution unlimited.

AFIT/GEP/PH/79D-9

HIGH TEMPERATURE HALL EFFECT IN INDIUM-DOPED SILICON.

Master's THESIS,

Presented to the Faculty of the School of Engineering
of the Air Force Institute of Technology
Air Training Command
in Partial Fulfillment of the
Requirements for the Degree of
Master of Science

by

Gary E. Rattray B.A.
Captain USAF
Graduate Engineering Physics

December 1979

85

Accession For
NTIS GRA&I
DDC TAB
Unannounced
Justification
By
Distribution/
Availability Codes
Dist. | Avail and/or special
A

Approved for public release; distribution unlimited.

012 225

Acknowledgements

I am indebted to many for their assistance in this project. Dr. Theodore Luke, my faculty advisor, deserves thanks for his timely advice. Several people with whom I worked in the Air Force Materials Laboratory contributed greatly. Dr. William Mitchel, National Research Council Fellow, was very generous with his suggestions. Dr. Steve Smith, University of Dayton Research Institute, assisted with the computer programs, and without the resourcefulness of Paul von Richter, UDRI, the experimental apparatus could not have been built. I would like to thank Dr. Joseph Lang, Thomas More College, for his insights into fitting theory and the use of his fitting program. In addition to these contributions, their companionship made the time spent on the work enjoyable. I am grateful to have been associated with Dr. Patrick Hemenger. His extensive knowledge, skillful assistance, and infinite patience made the completion of the project possible.

Contents

		Page
Acknowledgements		ii
List of Figures		v
List of Tables		vii
Abstract		viii
I.	Introduction	1
II.	Theory	4
	van der Pauw Measurements	4
	Resistivity	5
	Hall Mobility	6
	Carrier Concentration	7
	Charge Balance Equation	9
III.	Experimental Apparatus	15
	Oven	15
	Sample Holder	16
	Samples	18
	van der Pauw System	18
IV.	Experimental Approach	21
V.	Data Analysis	24
	Resistivity, Mobility, and Carrier Concentration	24
	Fitting Program	24
VI.	Results	28
	Testing of Apparatus	28
	Error Analysis	29
	Results of Data Reduction	32
	Sample 0145	32
	Sample 0151	33
	Sample 0288	35
VII.	Conclusions and Recommendations	38
Bibliography		40

Page

Appendix A: Results..... A1

Sample 0145..... A2
Sample 0151..... A10
Sample 0288..... A18

Appendix B: Derivation of Extrinsic Slope..... B1

Appendix C: Derivation of Error Due to Temperature..... C1

List of Figures

Figures		Page
1	Van der Pauw Sample.....	5
2	Hall Mobility Measurement.....	6
3	Energy Level Diagram for p-type Semiconductor..	9
4	Concentration as a Function of Temperature.....	14
5	Oven.....	16
6	Sample Holder.....	17
7	Van der Pauw Sample with Aluminum Film Contacts	18
8	Van der Pauw Positions.....	19
9	Van der Pauw System.....	19
10	Experimental Equipment.....	20
A1	0145 Resistivity Versus 1000/T.....	A3
A2	0145 Mobility Versus 1000/T.....	A4
A3	0145 Concentration Versus 1000/T.....	A5
A4	0145 Low Data, r=1.....	A6
A5	0145 All Data, r=1.....	A7
A6	0145 Low Data, Empirical r.....	A8
A7	0145 All Data, Empirical r.....	A9
A8	0151 Resustivity Versus 1000/T.....	A11
A9	0151 Mobility Versus 1000/T.....	A12
A10	0151 Concentration Versus 1000/T.....	A13
A11	0151 Low Data, r=1.....	A14
A12	0151 All Data, r=1.....	A15
A13	0151 Low Data, Empirical r.....	A16
A14	0151 All Data, Empirical r.....	A17

Figure		Page
A15	0288 Resistivity Versus 1000/T (High).....	A19
A16	0288 Mobility Versus 1000/T (High).....	A20
A17	0288 Concentration Versus 1000/T (High).....	A21
A18	0288 Resistivity Versus 1000/T (Low).....	A23
A19	0288 Mobility Versus 1000/T (Low).....	A24
A20	0288 Concentration Versus 1000/T (Low).....	A25
A21	0288 Low Data, r=1.....	A26
A22	0288 All Data, r=1.....	A27
A23	0288 Low Data, Empirical r.....	A28
A24	0288 All Data, Empirical r.....	A29

List of Tables

Table		Page
I	Comparison of Fitting Results.....	34
II	Sample 0145 High Temperature.....	A2
III	Sample 0151 High Temperature.....	A10
IV	Sample 0288 High Temperature.....	A18
V	Sample 0288 Low Temperature.....	A22

Abstract

Apparatus was designed and constructed to make resistivity and Hall coeffecient measurements at temperatures up to 875 degrees Kelvin. Data was taken on three indium-doped silicon samples, and resistivity, Hall mobility, and carrier concentration calculated for temperatures through the exhaustion region. The concentrations and activation energies of the various dopants were determined by fitting carrier concentration as a function of temperature to the charge balance equation. Four fits were made to the data from each sample. In order to determine the effect of assuming a Hall scattering factor (r-factor) of one, fits were made to low temperature data alone and then with the high temperature data added. The fits were also made using an empirical, temperature dependent formula for the Hall scattering factor. The results indicated that the temperature dependent r-factor gave better fits for each sample. The values for concentrations and activation energies were also in better agreement with values obtained from other experimental techniques.

I. Introduction

The purpose of this thesis is the characterization of the electrical properties of indium-doped silicon in the temperature range from 295 to 875 degrees Kelvin. The Air Force Materials Laboratory is engaged in the study of silicon:indium as a material for use in extrinsic infrared detectors. The characterization of the electrical properties is an integral part of that study.

Analysis of resistivity and Hall Effect measurements as functions of temperature provides one of the most useful techniques for determining the electrical properties of a semiconductor material. The resistivity and Hall mobility as functions of temperature can be calculated from the data. The ratio of Hall mobility to conductivity mobility is known as the Hall scattering factor (or r-factor). If it were known, the carrier concentration could be determined to within experimental error. The donor concentration, acceptor concentration, and acceptor activation energy can then be found by fitting the carrier concentration to the charge balance equation with a curve fitting computer routine.

Equipment for making the measurements from 20 to 400 K has been in operation in the Materials Laboratory for some time (Ref 3). However, since indium, as a dopant in silicon, has an activation energy of approximately 0.16ev, its exhaustion temperature may be as high as 700 degrees for heavily

doped samples. The relative error in the calculation of carrier concentration is at least as large as the relative error in the Hall scattering factor. The exact nature of the r-factor is not known, but it is usually close to one, and assuming it equal to one produces good results in temperature regions where the data is taken directly. However since the curve fitting routine uses the data to make a fit from zero degrees through the exhaustion region, an error in the low temperature region can be greatly magnified in the exhaustion region. This error can be reduced by making the measurements of the exhaustion region directly. Also, with the additional high temperature data, a temperature dependent model for the r-factor can be tested by comparing fits of carrier concentration calculated using it and values calculated using r equal to one.

Apparatus for making the measurements at temperatures up to 875 K was designed and constructed. Two samples with indium concentrations of approximately 2×10^{16} cm^{-3} and one with a concentration of 3×10^{17} cm^{-3} were analyzed. Four computer routine fits were made for each sample. The first was based on low temperature data and an r-factor of unity. The high temperature data was then added to determine its effect on the fit. A fit was then made using the low temperature data with the temperature dependent r-factor. Lastly, the high temperature data was added to this fit. Comparison showed that the temperature dependent r-factor yielded the better results.

The thesis is divided into six parts: (1) theory; (2) experimental apparatus; (3) experimental approach; (4) data analysis; (5) results; and (6) conclusions and recommendations.

II. Theory

The first part of this section shows the development of the equations for determining resistivity, Hall mobility, and free carrier concentration from the Hall data. In the second part, the charge balance equation used to determine concentrations and activation energies of the various dopants is developed.

Van der Pauw Measurements

The technique developed by van der Pauw for measuring resistivities and Hall co-effecients in lemellae of arbitrary shape permits the measurements to be made in a simpler manner than with the standard Hall bar approach. Proof of the theory is developed from conformal mapping of the arbitrary shap. (Ref 8) The samples used in this thesis are cut in a clover-leaf shape so that, with the proper switching arrangement, current can be applied between any two of the corners (Fig 1).

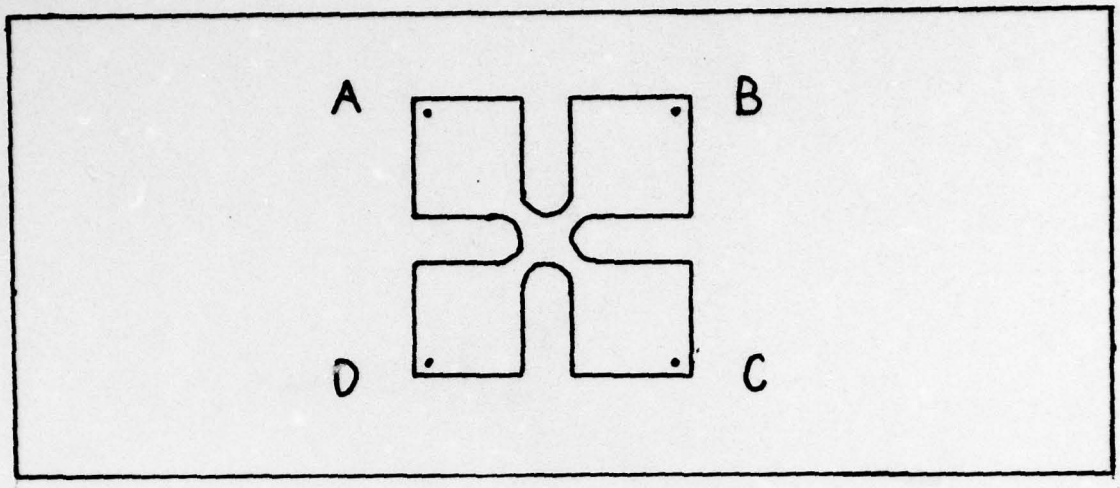

Figure 1 van der Pauw Sample

Resistivity. With a current applied between two adjacent corners, the resulting potential difference between the other two corners is measured. R_1 is then defined as the potential difference divided by the applied current. R_2 is obtained by applying the current in a direction orthogonal to the first measurement. R_1 and R_2 are related by Eq 1:

$$\exp\left(\frac{-\pi t R_1}{\rho}\right) + \exp\left(\frac{-\pi t R_2}{\rho}\right) = 1 \qquad (1)$$

where

is the thickness of the sample (cm)

is the resistivity of the material

Resistivity (in ohm-cm) is therefore defined by Eq 2:

$$\rho = f\left(R_1/R_2\right)\left(\frac{R_1 + R_2}{2}\right)\frac{\pi t}{\ln 2} \qquad (2)$$

$f(R_1/R_2)$ is a dimensionless function. When R_1 and R_2 are approximately equal, it may be expressed as:

$$f(R_1/R_2) = 1 - \frac{(R_2 - R_1)^2}{(R_2 + R_1)^2} \frac{\ln 2}{2} - \frac{(R_2 - R_1)^4}{(R_2 + R_1)^4} \left[\frac{(\ln 2)^2}{4} - \frac{\ln 2}{2} \right] \quad (3)$$

Hall Mobility. Mobility is determined in the following manner. A current is applied between diagonally opposite corners, and the voltage difference between the other two corners is measured. The measurement is then repeated with a magnetic field applied perpendicular to the sample. The difference between the two values obtained by dividing the voltages by the applied currents is called R_1 and for the configuration shown in Fig 2, is given by:

$$\Delta R = \left| \frac{V_a(0) - V_c(0)}{I_{bd}(0)} - \frac{V_a(\bar{B}) - V_c(\bar{B})}{I_{bd}(\bar{B})} \right| \quad (4)$$

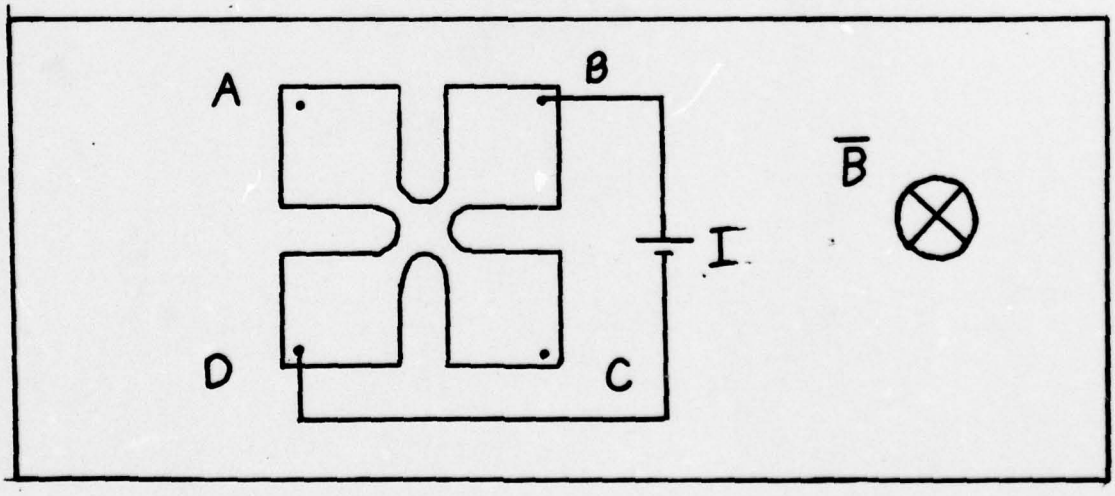

Figure 2 Hall Mobility Measurement

The Hall mobility (in cm^2/volt-sec) is given by (Ref 7:4):

$$\mu_H = \frac{10^8 \Delta R}{\rho B t} \tag{5}$$

where

B is the magnetic field (gauss)

Carrier Concentration. The resistivity of a material is defined by:

$$\frac{1}{\rho} = pe\mu_{cp} + ne\mu_{ce} \tag{6}$$

where

p is the hole carrier concentration

n is the electron carrier concentration

μ_{cp} is the hole conductivity mobility

μ_{ce} is the electron conductivity mobility

For a sample heavily doped with an acceptor impurity, this reduces to:

$$\frac{1}{\rho} = pe\mu_{cp} \tag{7}$$

The hole carrier concentration is therefore given by:

$$p = \frac{1}{\rho e \mu_{cp}} \tag{8}$$

As shown above, the resistivity and Hall mobility are determined from the measurements. In general, the Hall

mobility is not equal to the conductivity mobility. The ratio, $r=\mu_H/\mu_c$, is known as the r-factor (or Hall scattering factor). If the r-factor is known, the carrier concentration can be determined to within experimental error;

$$p = \frac{r}{\rho q \mu_H} \tag{9}$$

Unfortunately, an exact function for r has not yet been determined. It is usually close to one, and is set equal to one in most analyses in order to facilitate the calculation of hole concentration. It is, however, dependent upon scattering mechanisms and band shapes, and therefore changes with temperature and dopant concentration (Ref 6). Baron et al, report a value of 0.69 for an indium-doped silicon sample with an indium concentration of 3×10^{17} cm^{-3} at 600 degrees Kelvin (Ref 1:26). An "empirical" function for the r-factor developed by Dr. Joseph Lang is shown as Eq 10 (Ref 4):

$$r(T) = 0.54 + \frac{1.22T}{50\left(1+\frac{T^2}{50^2}\right)} \tag{10}$$

This model is built upon scattering theory and data and was adjusted to yield best fits for shallow (low activation energy) p-type dopants in silicon. It should be noted that it has temperature dependence, but no dopant concentration dependence. Both theoretical and experimental work on the exact nature of the r-factor is under way at the Air Force Materials Laboratory.

Charge Balance Equation

Intrinsic silicon is an n-type semiconductor due to the greater mobility of the electrons in the conduction band. While the production of pure silicon is not possible, material can be doped in such a manner that the donor and acceptor concentrations are equal. Such material is termed "compensated" and behaves as intrinsic silicon would. Doping with indium, a group III element, lowers the Fermi level so that the hole carrier concentration becomes greater than the electron carrier concentration. In terms of an energy level diagram, the indium atoms in substitutional positions may be considered to create an acceptor level lying approximately 0.16ev above the valence band (Fig 3).

At absolute zero, the Fermi level, E_f, lies halfway between the valence band and the acceptor level. As the

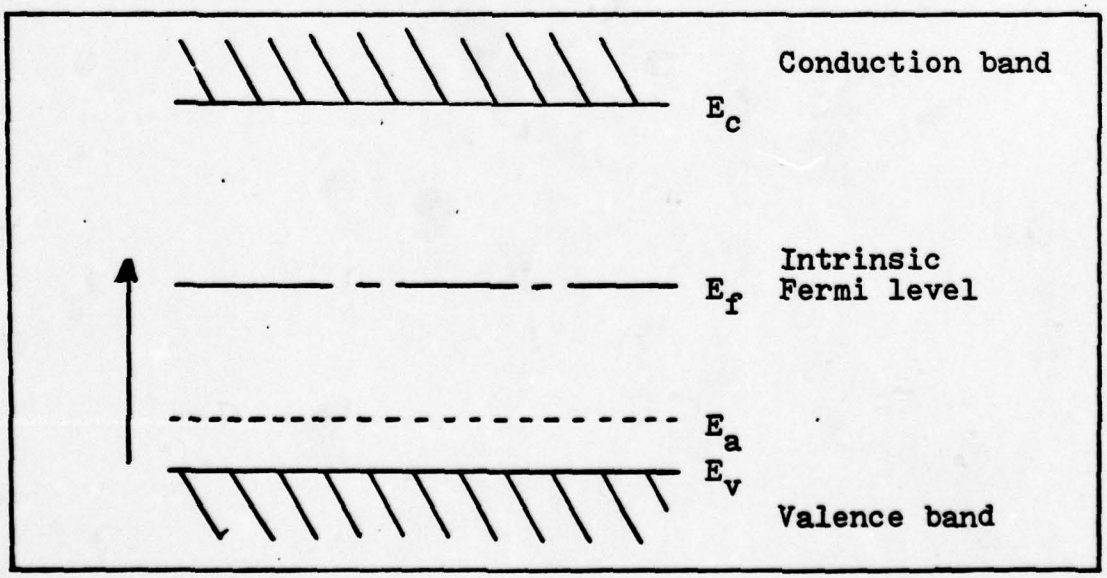

Figure 3 Energy Level Diagram for p-type Semiconductor

temperature increases, E_f first falls slightly and then rises. At very high temperatures it approaches the intrinsic Fermi level, and the electrical behavior of the material becomes intrinsic. With higher dopant densities, higher temperatures are required to cause the Fermi level to approach the intrinsic Fermi level. (Ref 5:276)

The intrinsic hole concentration can be calculated by multiplying the energy density of states by the Fermi-Dirac probability function for holes and integrating over the range from the bottom to the top of the valence band. When E_v is set equal to zero as a reference and E_f is greater than kT, the approximate result is (Ref 5:265):

$$p = \frac{2(2\pi m_h^* kT)^{3/2}}{h^3} \exp \frac{-E_f}{kT} \qquad (11)$$

where

m_h^* is the effective mass for holes

h is Planck's constant

k is Boltzmann's constant

T is temperature (degrees Kelvin)

and

E_f is the Fermi level energy

The Fermi-Dirac function for acceptor levels as developed by Putley is valid if the acceptor is in the ground state (Ref 6:123):

$$f(E_a) = \frac{1}{1 + \frac{1}{g} \exp \frac{E_f - E_a}{kT}} \qquad (12)$$

where

E_a is the acceptor energy level

g is the degeneracy of the acceptor state

The concentration of holes associated with acceptor atoms is equal to the concentration of acceptors, N_a, multiplied by Eq (12). The charge balance equation states that the total positive charge must equal the total negative charge:

$$p + N_d - n_d = n + N_a - p_a \qquad (13)$$

where

N_d is the donor concentration

n_d is the unionized donor concentration

n is the election carrier concentration

p_a is the unionized acceptor concentration

For N_a much greater than N_d, all the donors will be ionized so that n_d equals 0. For extrinsic conduction, hole carrier concentration is much greater than electron carrier concentration and n can be dropped from Eq (13). The concentration of unionized acceptors is N_a multiplied by Eq (12), the probability of the hole being associated with the acceptor atom. Eq (13) may then be rewritten:

$$p + N_d = N_a - \frac{N_a}{1 + \frac{1}{g} \exp \frac{E_f - E_a}{kT}} \qquad (14)$$

Solving Eq (11) for E_f/kT and substituting into Eq (14) yields:

$$p + N_d = \frac{N_a}{1 + \frac{pg}{N_F} \exp \frac{E_a}{kT}} \qquad (15)$$

where

$$N_F = \frac{2(2\pi m_h^* kT)^{3/2}}{h^3} \qquad (16)$$

This equation is easily generalized to enclude several acceptor levels:

$$p + N_d = \sum_i \frac{N_{a_i}}{1 + \frac{pg_i}{N_F} \exp \frac{E_{a_i}}{kT}} \qquad (17)$$

This form of the charge balance equation is especially useful because it expressed the carrier concentration as a function of temperature, but not explicitly as a function of the Fermi level.

In the case of low temperatures such the $E_a \gg kT$, Eq (14) reduces to:

$$p = \frac{(N_a - N_d)}{N_d} \frac{N_F}{g} \exp \frac{-E_a}{kT} \qquad (18)$$

For the special case that N equals N_a:

$$p = \left(\frac{N_a N_v}{g}\right)^{1/2} \exp \frac{-E_a}{2kT} \qquad (19)$$

At high temperatures where $E_g \gg kT \gg E_a$,

$$p = N_a - N_d \qquad (20)$$

Fig 4 shows the characteristic curve obtained when ln p is plotted versus 1/T. In the low temperature region, the slope is either E_a or $E_a/2$ depending on whether Eq (18) or Eq (19) applies. At high temperatures all the acceptors become ionized, and the slope becomes zero. This is known as the exhaustion region. At still higher temperatures, the conduction due to intrinsically generated carriers becomes predominant, and the slope is approximately equal to one-half the energy gap between the conduction and valence bands.

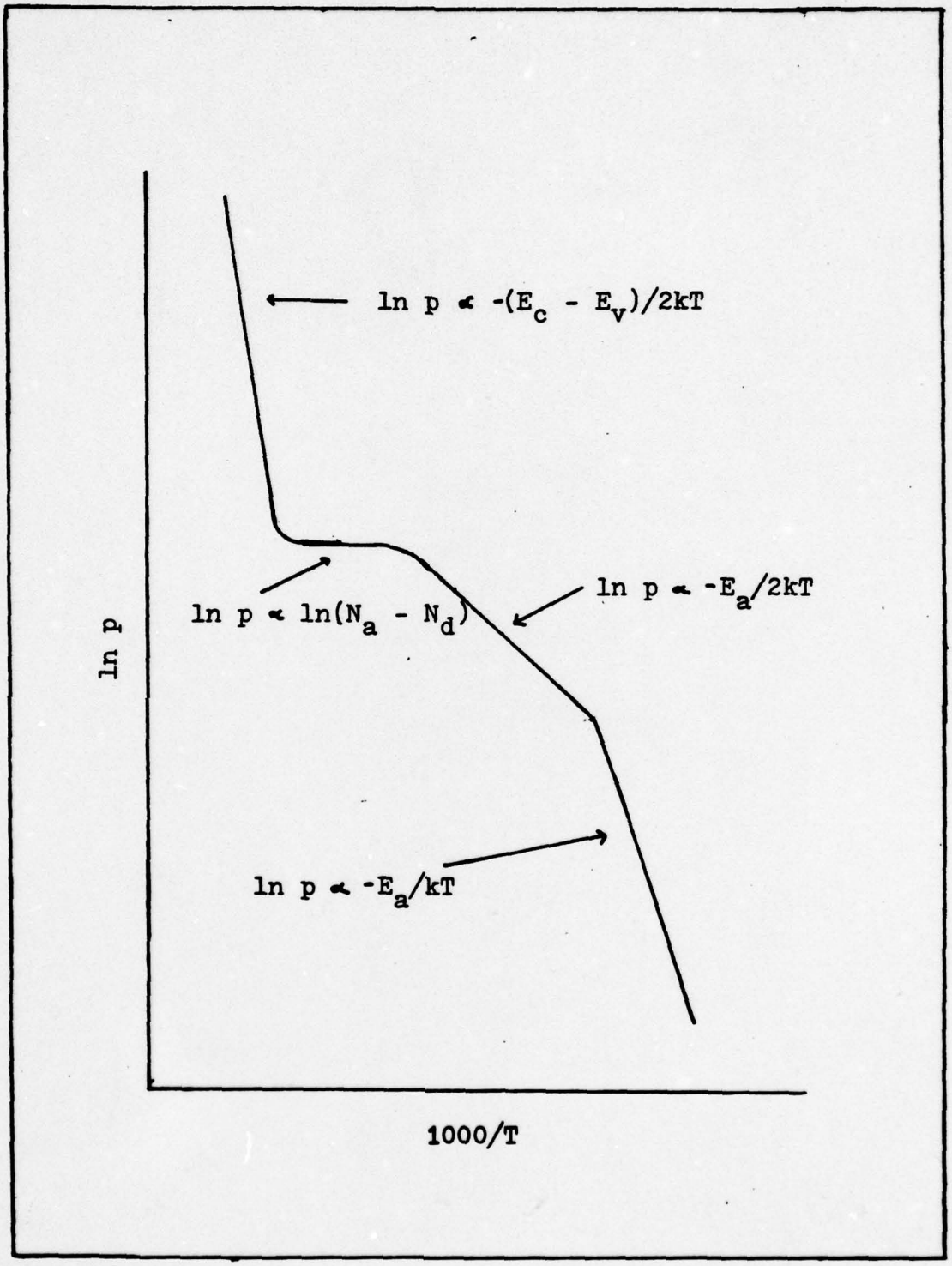

Figure 4 Concentration as a Function of Temperature

III. Experimental Apparatus

The experimental work done was essentially the classical Hall experiment. The difficulties which had to be overcome were associated with constructing the apparatus to operate at temperatures up to 875 degrees Kelvin. Since the melting points of most solders and epoxies are well below this temperature, mechanical connections were used. Argon gas was passed over the sample during heating to minimize oxidation processes. Also, care was taken to ensure that no materials were used which might alter the uniformity of the magnetic field.

This section describes the oven and sample holder. The sample and van der Pauw system are also discussed.

Oven

The heating component of the oven is a ceramic tube wound with resistive heating wire and insulated with asbestos. A quartz tube which fits inside the heater is closed on one end and has an inlet and an outlet for the argon gas. It is operated vertically with the top closed by a rubber stopper. The thermocouple leads and sample contact wires are contained in thermocouple tubing extending through the rubber stopper. Also, the stopper supports a stainless steel rod which, in turn, supports the sample holder. Access to the sample holder is obtained by removing the stopper, rod, and sample holder as one piece.

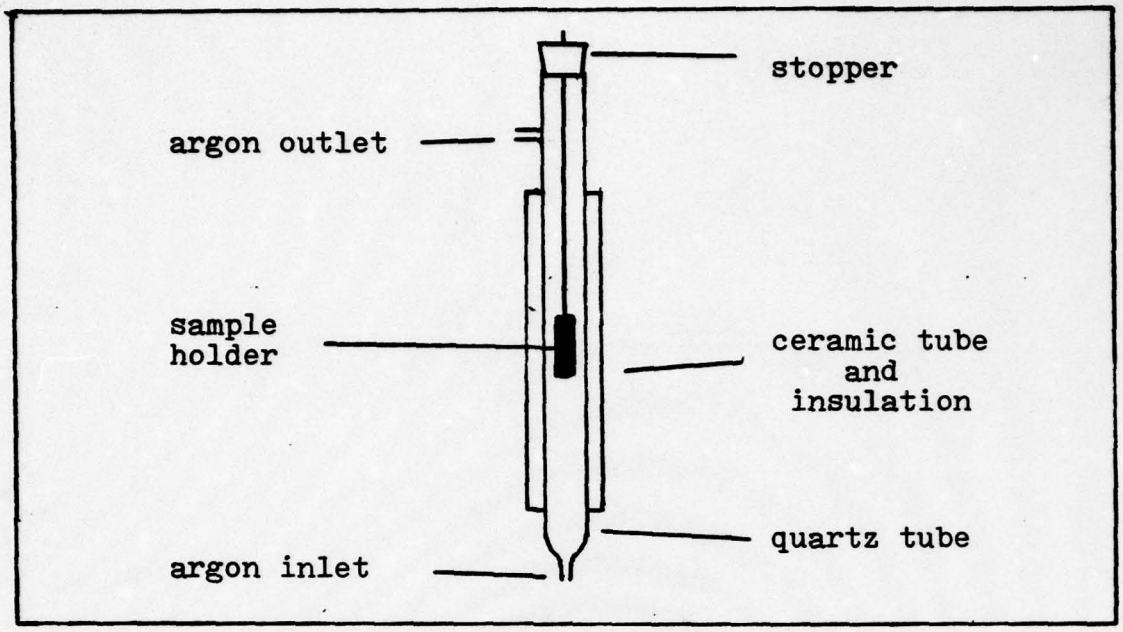

Figure 5 Oven

Temperature control is effected by an on-off thermostat control with a Chromel-Alumel thermocouple located between the ceramic and quartz tubes providing the feedback. A Variac placed in series between the controller and heater allows for use of smaller heating currents at lower temperatures.

Sample Holder

The main body of the sample holder is a copper block which serves as a platform for mounting the sample, connections, and thermocouple. Due to its large thermal mass, it also increases temperature stability. The sample is mounted on a wafer of beryllium oxide, an electrical insulator and thermal conductor. The center of the copper block is cut out, and brass bolts are used to "sandwich" the block between two

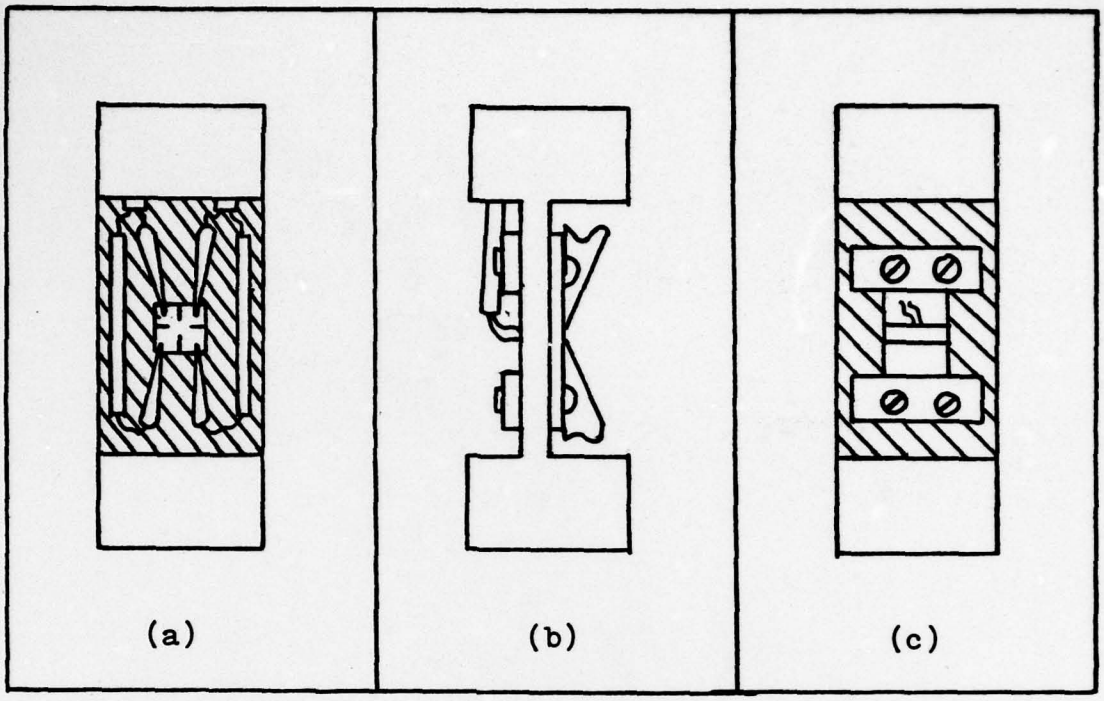

Figure 6 Three Views of Sample Holder; (a) Front, (b) Side, and (c) Rear

wafers of beryllium oxide. Besides securing the wafer to the block, the bolts hold the stainless steel clips which contact the corners of the sample. The clips provide both electrical contact and mechanical support to the sample. Copper wires run from the bolts out through ceramic thermocouple tubing.

Sample temperature is measured by a Chromel-Alumel thermocouple located on the reverse side of the wafer on which the sample is mounted. The sample holder is enclosed in a copper sleeve which acts as a radiation shield.

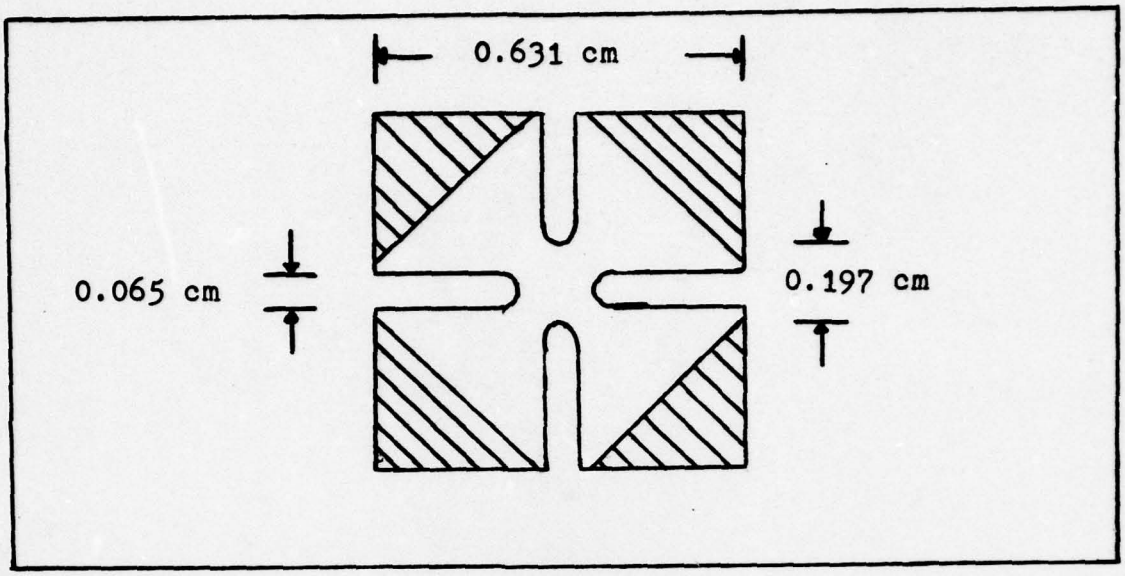

Figure 7 van der Pauw Sample with Aluminum Contacts

Samples

The samples are cut in the "clover-leaf" shape with an ultrasonic cutter. Sample dimensions are shown in Fig 7; thicknesses range from 0.071 cm to 0.091 cm. The contact areas have a thin film of aluminum, a group III element with an activation energy less than that of indium, evaporated onto them.

Van der Pauw System

The van der Pauw measurements described in section II require a switching arrangement to change the current and voltage leads. The six van der Pauw positions are shown in Fig 8, and the experimental system is shown in Fig 9 Ref 4:698). The configuration shown in Fig 9 corresponds to positions (b) of Fig 8, but all six positions can be achieved by means of the six-section six-position rotary switch.

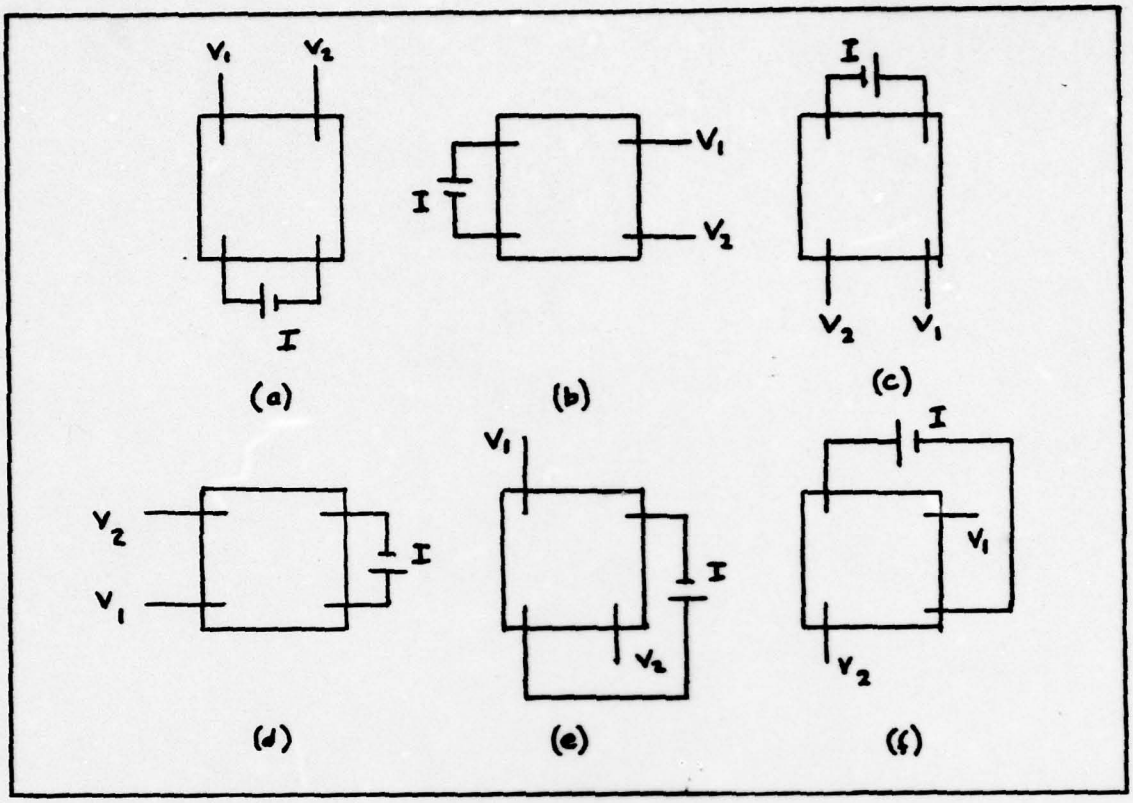

Figure 8 van der Pauw Positions (Ref 3:698)

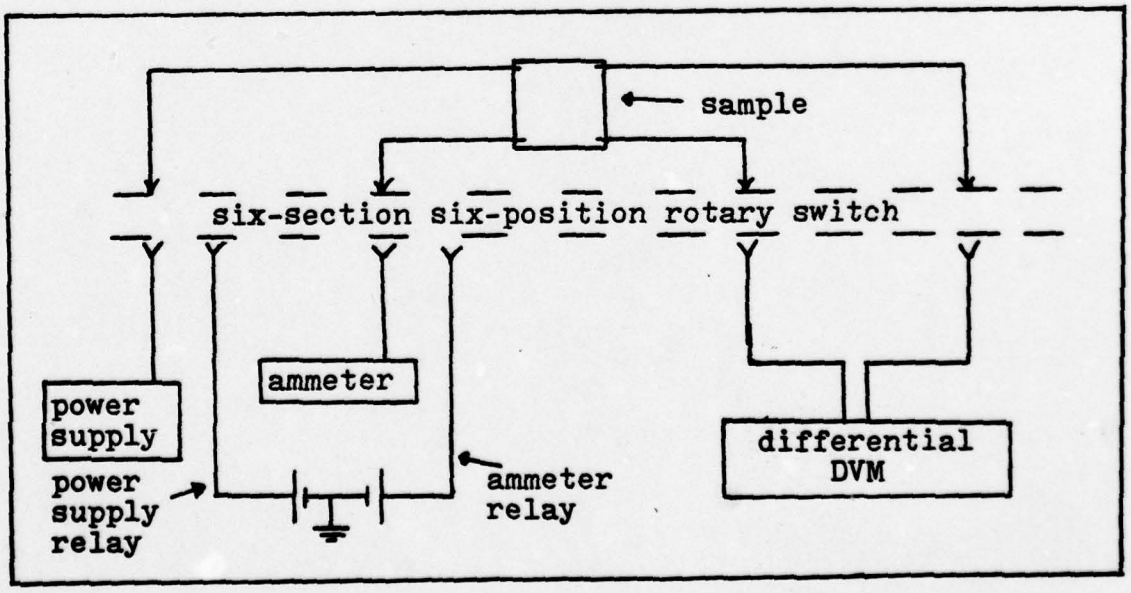

Figure 9 van der Pauw System

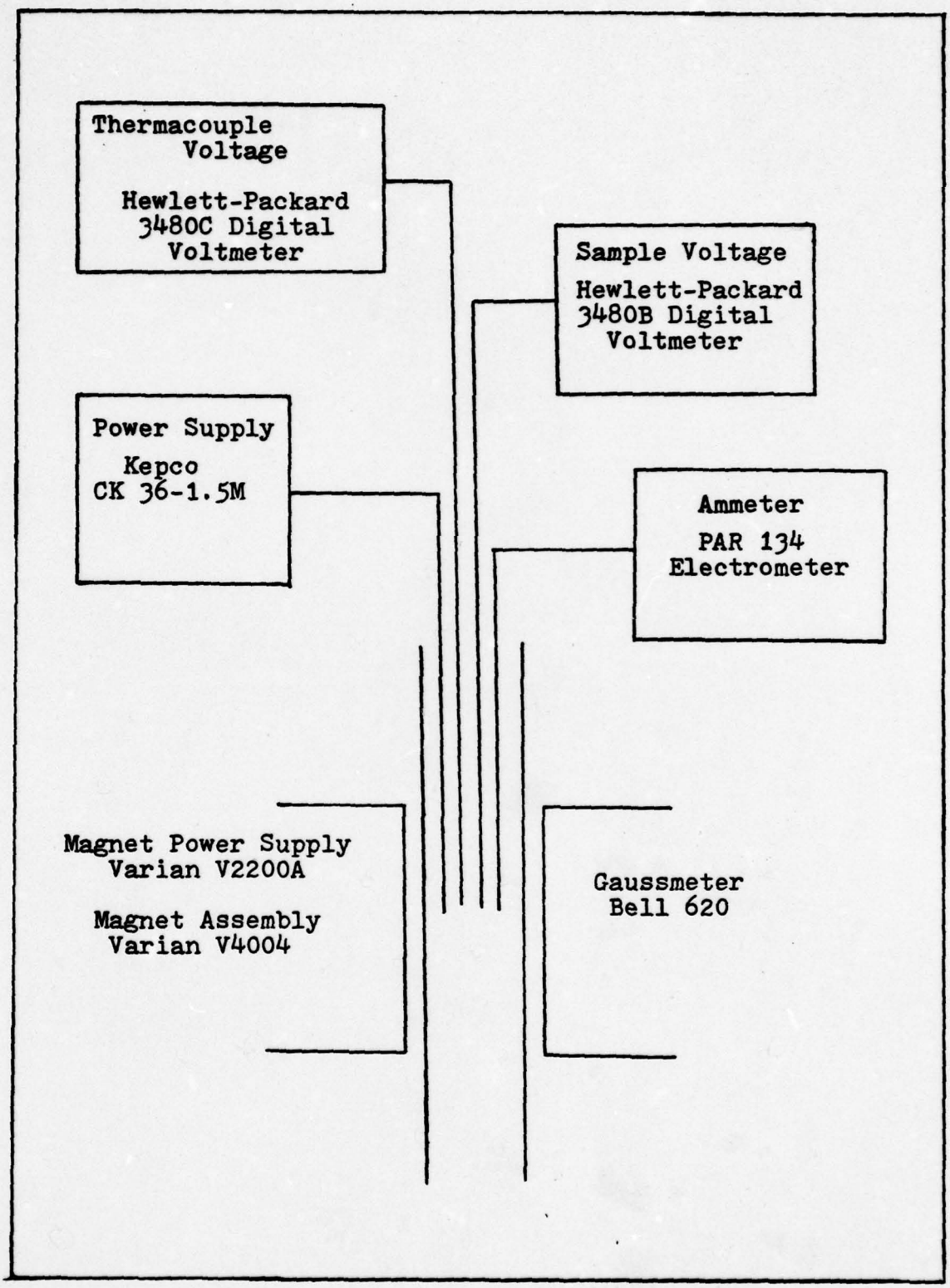

Figure 10 Experimental Equipment

IV. Experimental Approach

After the sample is mounted in the holder, the contacts are checked to ensure that their resistances are approximately equal and ohmic. For a given voltage applied across the sample, the current should be the same in each of the six van der Pauw positions, and with the current in either direction. The contacts are ohmic if an increase in the applied current results in a proportionate increase in the measured potential difference.

The sample holder is then positioned in the oven so that the sample face is perpendicular to the direction of the magnetic field. A high flow rate (approximately 20 cubic feet per hour) of argon gas is used to purge the oven. This prevents oxidation of the sample and the sample holder components. After five minutes the flow rate is cut back to maintain a slight positive pressure. The argon entering from the bottom results in a slow, uniform diffusion up around the sample. Approximately 5 cubic feet per hour is sufficient to prevent oxidation at temperatures up to 700 degrees Kelvin, but higher flow rates are necessary above that temperature.

The desired temperature is set on the thermostat, and the system allowed to come to equilibrium. Since the heating is essentially radiative and the copper sample holder has a large mass, the process is quite slow. The time required may be decreased by first heating the ceramic portion of the

oven to a higher temperature, and then setting the thermostat at the desired temperature.

Data from van der Pauw positions 1, 2, and 5 or from 3, 4, and 6 is sufficient to make the resistivity, mobility, and carrier concentration calculations. To eliminate possible errors associated with achieving an exactly zero magnetic field, the readings for positions 5 or 6 are made with the field in both normal and reverse polarity. The absolute difference between the two values obtained is divided by two to obtain the ΔR used in Eq (5). Also, the readings for all the measurements are made with the current applied in both forward and reverse directions. With the data taken for each set of positions and with the current in each of the two possible directions, four independent sets of data are obtained for each temperature point.

Data points are spaced approximately 50 degrees apart. Calculated values are usually plotted versus inverse temperature. Since 1/T varies slowly with respect to T at large temperatures, it is not necessary to make the data points any closer together.

The computer routine used to match carrier concentration to the charge balance equation assumes only extrinsic conduction. Therefore it is not necessary to take data above the exhaustion region except to ensure that exhaustion has indeed been reached. High temperatures may result in activating oxygen atoms and cause other changes in the sample. To avoid unnecessarily high temperatures, the concentration is

calculated and plotted during the run. Once the behavior becomes intrinsic, the sample is allowed to cool, and the room temperature measurements are repeated to ensure the characteristics have not been changed by the high temperatures.

V. Data Analysis

The first part of this section describes the computation of resistivity, mobility, and free carrier concentration. The second part discusses the program used to obtain the concentrations and activation energies of the dopants.

Resistivity, Mobility, and Concentration

A computer program is used to calculate resistivity, mobility and carrier concentration using Eq (2), (5), and (9) with an r-factor of one. Each of the four independent sets of data is treated separately so that four values of each characteristic are obtained at each temperature point. The program averages the values for forward and reverse current and makes plots versus inverse temperature. The two values at each temperature point represent the two sets of switch positions.

Fitting Program

This routine uses a least squares fitting technique to fit carrier concentration and temperature to the charge balance equation:

$$p + N_d = \sum_i \frac{N_{a_i}}{1 + \frac{p g_i}{N_F} \exp \frac{E_{a_i}}{kT}} \qquad (17)$$

The carrier concentration (calculated from Eq (9)) and the corresponding temperature are fed into the computer with

estimates of the donor concentration (N_d) and the acceptor concentration (N_a), activation energy (E_a), and degeneracy (g) for each acceptor level. Each of these estimated values may be fixed or allowed to vary. In this thesis the degeneracies are assigned their "known" values, and the other parameters are allowed to vary. The computer routine adjusts these parameters through several iterations to arrive at values for which the p(T) calculated from Eq (17) best fits the input data points. The printout contains the values which yield the best fit, and it shows the per cent difference between the experimental concentration and the p(T) calculated from the best fit parameters at each experimental data point. A plot of ln p versus 1000/T showing the experimental points and p(T) is also generated.

As was noted previously, the program assumes only extrinsic conduction and so extends the exhaustion plateau to infinite temperature. The program can be used to fit concentration up to the exhaustion region based only on data from temperatures below the exhaustion region. This was necessary for indium-doped silicon studies in the Materials Laboratory prior to the experimental work this thesis represents.

The program has the capability of using the concentration as computed with an r-factor of one or adjusting the concentration by r(T) as the data is read in. Where r(T) is given by:

$$r(T) = 0.54 + \frac{1.22\,T}{50\left(1 + \frac{T^2}{50^2}\right)} \qquad (10)$$

This thesis uses the fitting routine with each r-factor in computing concentrations and activations from the low temperature alone, and then makes the same two fits with the new data from the exhaustion region added. This is done to determine and reduce the error caused by extrapolation from low temperature data and to test the empirical r(T) given by Eq (10).

VI. Results

This section is divided into three parts. The first describes the testing of the designed equipment. Next, the relative error in the calculated concentrations is discussed. The last part is an analysis of the results of the data reduction.

Testing of Apparatus

The apparatus was first tested at room temperature to ensure that the electrical contacts to the sample worked properly. The contacts proved to be ohmic, and for a constant power supply voltage, current through the sample was approximately equal in each van der Pauw position and in each direction. The stainless steel clips were removed, and gold wires attached to the contact areas as used in the low temperature system. Measurements proved to be the same in each arrangement. The stainless steel clips were later found to be slightly magnetic and were replaced with clips fashioned from a Columbium alloy. Again, the Hall measurements showed no change, so the stainless steel was used because of its higher resistance to oxidation. The last check was the rotation of the sample in the holder by 90 degrees. As expected, the ratio of R_1 to R_2 was inverted, and the measurements were otherwise unchanged.

A high temperature run was then begun on an indium-doped test sample. Exhaustion was reached at about 500

degrees Kelvin with a concentration of 10^{17} cm^{-3}. At temperatures above 650K, the sign of the Hall signal was reversed indicating that the sample had become n-type. The sample was run to 760K, and then allowed to cool to room temperature, where measurements following the run showed the sample characteristics to be unchanged.

The first attempt to run the apparatus to its design limit of 875 degrees was unsuccessful. Above 750 degrees the contact performance became unsatisfactory. The run was continued with the oven and temperature control working well. Upon return to room temperature, the contact problem persisted, and the aluminum coating on the contact areas showed signs of oxidation. A second run with the argon flow doubled above 700 degrees resulted in good operation of the system through the entire temperature range.

Error Analysis

If the expressions for ρ and μ are substituted into Eq (9) and like terms cancelled:

$$\rho = \frac{Br\,10^{-8}}{\Delta Ret} \tag{21}$$

In terms of measured values this is:

$$\rho = \frac{Br\,I_H\,10^{-8}}{V_H\,et} \tag{22}$$

where

I_H is the applied current

V_H is the voltage change due to the magnetic field.

Therefore, the relative error in ρ due to errors in measurements is:

$$\frac{\Delta\rho}{\rho} = \left[\left(\frac{\Delta B}{B}\right)^2 + \left(\frac{\Delta I_H}{I_H}\right)^2 + \left(\frac{\Delta V_H}{V_H}\right)^2 + \left(\frac{\Delta t}{t}\right)^2\right]^{1/2} \qquad (23)$$

The magnetic field, applied current, and sample thickness can all be measured to within one per cent. The Hall voltage, V_H, cannot be determined as precisely. The Hall coefficient is defined by:

$$R_H = \frac{V_H \, 10^8}{I_H B} \qquad (24)$$

The Hall voltage is:

$$V_H = R_H I_H B \, 10^{-8} \qquad (25)$$

For high concentration samples, the Hall coefficient becomes very small at high temperatures. The magnetic field strength is limited to four kilogauss by the pole separation necessary to accomodate the oven. Therefore, the only way to increase the Hall voltage is by increasing the current. Care must be exercised, however, to avoid Joule (I^2R) heating of the sample. This would result in the sample temperature being higher than that registered by the thermocouple, and would

cause an artificially high concentration value. With these limitations, the error in the voltage reading varies from about three per cent at room temperature to about six per cent in the exhaustion region. It becomes even higher in the intrinsic region, but these values are not used in the curve fitting routine. From Eq (23) the relative error due to errors of measurement is dominated by the voltage uncertainty and varies from about three per cent to six per cent depending on temperature.

There is also a source of error due to the dependence of carrier concentration on temperature. The region of interest with the greatest temperature dependence is the region dominated by the $E_a/2$ slope. The relative error is shown in Appendix C to be:

$$\frac{\Delta\rho}{\rho} = \left[\frac{3}{4} + \frac{E_a}{2kT}\right]\frac{\Delta T}{T} \qquad (26)$$

It is readily seen that the error decreases with temperature. The Chromel-Alumel thermocouple used is accurate to within three degrees. Therefore, the maximum error at 300 degrees is 4.75 per cent. As a test of the thermocouple accuracy, the sample was left in an isothermal enclosure with a mercury thermometer and a sample holder with a silicon diode thermometer. The temperature difference between any two was no greater than 0.75 degrees. Therefore, the relative error due to the temperature reading is probably less than two per cent.

The results of the data analysis are shown in Appendix A. Comparison of the two values reported for each data point shows that they never differ by more than five per cent for points below the intrinsic region.

Results of Data Reduction

Appendix A shows the results of the calculations. The table for each sample shows the resistivities, mobilities, and free carrier concentrations based on an r-factor of unity. Following the table are the three plots of these quantities versus 1000/T. The final four plots are the results of curve fitting to determine activation energies and donor and acceptor concentrations. The first fit is made with r equal to one and with low temperature data only. The second includes the high temperature data. The carrier concentrations are computed from low temperature data using the empirical r-factor given by Eq (10) for the third fit, and the last plot shows the result obtained using all data with the empitical r-factor. Table I is a comparison of the activation energies and donor and acceptor concentrations obtained from the four fits to each sample. The chi squared per degree of freedom, χ^2, is a relative measure of the quality of the fit. Except where otherwise stated, carrier concentrations are based on an r-factor of one.

Sample 0145. This sample was projected from analysis of low temperature data to contain about 5×10^{16} cm^{-3} indium and 10^{13} cm^{-3} aluminum. Exhaustion actually occurred at 480

degrees Kelvin with a free carrier concentration of about 3.8×10^{16} cm^{-3}. Examination of the results show the resistivity to be on the order of 1 ohm-cm with the minimum at just above room temperature. Hall mobility decreases with increasing temperature and is approximately 100 cm^2/volt-sec.

Comparison of curve fitting results shows much better agreement between low data alone and the combined data if the empirical r is used. Indium concentration from a fit of all data is about 13 per cent lower then that projected from low temperature data when the r-factor is assumed to be one. Table I shows that the difference between the two is almost non-existent if the empirical r-factor is used. Also, the chi squared per degree of freedom is much lower in the fits made using the empirical r.

Sample 0151. This sample was cut from the same boule as sample 0145. It exhausted at about 440 degrees and a concentration of 3.0×10^{16} with the exhaustion temperature being lower due to the smaller concentration. Hall mobility and resistivity were approximately the same as in sample 0145.

Examination of the curve fitting results reveals little change from the previous sample. The larger χ^2 is due to the deviation in the lowest temperature point. That point causes the low temperature slope to be shallower, and yields a low value of 0.068 ev for the aluminum activation energy. The quality of the fit remains better when the empirical r is used.

Comparison of Fitting Results

Table I

	r equal to one		empirical r	
	low T only	all data	low T only	all data
0145				
N_d	5.19E+12	5.06E+12	4.54E+12	4.53E+12
N_{In}	5.28E+16	4.67E+16	2.87E+16	2.87E+16
E_{In}	0.164	0.161	0.159	0.159
N_{Al}	1.24E+13	1.22E+13	1.26E+13	1.26E+13
E_{Al}	0.069	0.069	0.070	0.070
χ^2	1.7	2.1	1.6	1.4
0151				
N_d	1.07E+13	1.04E+13	9.30E+12	9.42E+12
N_{In}	3.98E+16	3.74E+16	2.16E+16	2.26E+16
E_{In}	0.163	0.162	0.158	0.158
N_{Al}	1.53E+13	1.49E+13	1.42E+13	1.44E+13
E_{Al}	0.068	0.068	0.068	0.068
χ^2	3.9	3.3	3.7	2.8
0228				
N_d	6.20E+13	1.27E+14	6.91E+13	9.14E+13
N_{In}	8.15E+17	5.70E+17	3.39E+16	2.95E+16
E_{In}	0.166	0.160	0.157	0.155
N_X	5.41E+13	1.02E+14	4.95E+13	6.04E+13
E_X	0.101	0.096	0.101	0.099
χ^2	0.9	3.6	0.8	1.0

Sample 0288. This sample was cut from a wafer supposed to contain about 5×10^{17} cm^{-3} indium. It was run first on the high temperature apparatus. Indium solder was then used to attach gold wires to the aluminum contact pads, and the sample run on the low temperature apparatus described in Ref 3.

Exhaustion occurred at about 600 K with a carrier concentration of 3.5×10^{17} cm^{-3}. Low temperature data revealed the presence of the X-level acceptor first reported by Baron, et.al. (Ref 1:24). This is an indium associated acceptor of uncertain origin. Resistivity varies from greater than 10^6 ohm-cm at 60 degrees Kelvin to a minimum of 0.3 ohm-cm at 425 degrees. Hall mobility decreases from greater than 10^3 cm^2/volt-sec to 20 cm^2/volt-sec at 746 degrees, the highest temperature measured.

Due to the greater range over which the low temperature data must be extrapolated, the difference between measured values and the concentration determined from fitting the low temperature data is greatly magnified. The experimental exhaustion is less than one half the predicted 8.15×10^{17}. When the empirical r-factor is used, the fits from all data and from low temperature data alone are in much better agreement. A comparison of the χ^2's for fits of all data using the two r-factors, shows a χ^2 of 3.6 for r equal to one and 1.0 for the empirical r.

To summarize, the value for carrier concentration determined from Hall Measurements will always be in error by at

least the uncertainty in the r-factor, the ratio of Hall mobility to conductivity mobility. While assuming r equal to one will usually result in an error of no greater than about 30 per cent, it is magnified when the low temperature data alone is used to obtain a fit to a sample with a high temperature exhaustion. There are, therefore, two errors associated with the uncertainty in r when determining indium concentration; one from the actual uncertainty at a given temperature, and the other caused by the propogation of the error from lower temperature data. Determination of the carrier concentration in the exhaustion region directly from Hall measurements lessens the propogation of error from low temperature data. As seen in Fig A22, however, the best fit curve still is above the high temperature points, and the over all quality of the fit is poor. Even if it were possible to obtain a perfect fit, the concentration would still be in error by the ratio of μ_H to μ_C at that temperature.

The fact that the fits for all temperature data and low temperature data alone yield similar results when the empirical r-factor is used shows that it is at least approximately correct. Another supporting argument is that the activation energy for indium is in much better agreement with its optically determined value of 0.155 ev.

The temperature dependence of the empirical r was developed from scattering data and by fitting data from samples doped with impurities which reach exhaustion in the low temperature region. It appears to be at least approximately

correct at temperatures up through the indium exhaustion temperature, and certainly yields better results than assuming the Hall mobility and conductivity mobility to be equal.

VII. Conclusions and Recommendations

The apparatus may be concluded to fulfill the purpose for which it was designed. Temperature control is good throughout the range from 295 to 875 K. The resistivity and Hall measurements are reproducible, and the data is self-consistent.

The major drawback to the set up is the long time required for the temperature to stabilize at each new data point. The time required could be shortened by wrapping heating wire around the ends of the sample holder and adding another thermocouple for feedback. The oven could then be held at a temperature lower than the desired sample temperature, and a temperature controller used to regulate heating current in the wire. This arrangement should lead to savings of time in data collection and to more precise temperature control and selection of data points.

Carrier concentrations measured directly in the exhaustion region are smaller than those predicted by fitting the low temperature data when the r-factor is assumed to be unity. If the empirical r-factor is used in calculating the carrier concentrations, however, the high temperature measurements agree well with the predictions based on low temperature data. Experimental and theoretical work is under way to determine the exact nature of the r-factor, and the fact that the experimental results of this thesis support the empirical r-factor indicates that the research is proceeding in the

correct direction. In the meantime, carrier concentrations may be determined more accurately using the empirical r-factor rather than an r-factor of unity. Acceptor concentrations, acceptor activation energy levels, and donor concentrations may then be determined quite accurately from low temperature data alone.

As noted previously, the fitting program assumes only extrinsic conduction. However, the exhaustion region of silicon-doped indium is at a high enough temperature that intrinsic conduction is noticably present. This is evident from the fact that the exhaustion region is a sort of shoulder rather than a flat plateau. Inclusion of the intrinsic term in the fitting program would result in a more realistic fit of the data to the curve. The calculated carrier concentrations from data points up through the exhaustion range could be included in the fit. A prerequisite to the inclusion of the intrinsic election carrier concentration is the calculation of the electron density of states effective mass for silicon.

Finally, the apparatus may prove useful in the analysis of thallium-doped silicon. Thallium has an activation energy, and therefore an exhaustion temperature, higher than that of indium. The system has been tested at temperatures up to 875 K and is limited by the 933K melting point of the aluminum used to coat the contact areas of the sample. Carrier concentrations measured at these high temperatures should provide valuable data in the thallium study.

Bibliography

1. Baron, R.,M.H. Young, J.P. Baukus, O.J. Marsh, and M.J. Sheets. "Properties of Indium-Doped Silicon as an Extrinsic Detector Material," paper presented at the IRIS Specialty Group Meeting on Infrared Detectors, U.S. Air Force Academy, Colorado, Mar 22-23, 1977.

2. Dobbs, B.C., P.M. Hemenger, and S.R. Smith. "Ohmic Contacts on High-Purity p-type Silicon," Journal of Electronic Materials, 6 (6): 705-714 (Apr 1977).

3. Hemenger, P.M. "Measurement of High Resistivity Semiconductors Using the van der Pauw Method," Review of Scientific Instruments, 44 (6): 698-700 (Jun 1973).

4. Lang, J.E. Professor, Physics Department, Thomas More College (Personal Communication). Fort Mitchell, Kentucky, Aug 1979.

5. McKelvey, J.P. Solid State and Semiconductor Physics. New York: Harper and Row, 1966.

6. Putley, E.H. The Hall Effect and Semiconductor Physics. New York: Dover Publications, Inc. 1968.

7. van der Pauw, L.J. "Methods of Measuring Specific Resistivity and Hall Effects of Discs of Arbitrary Shape," Phillips Research Reports, 13: 1-9 (Feb 1958).

8. van der Pauw, L.J. "A Method of Measuring the Resistivity and Hall Coefficient of Lamellae of Arbitrary Shape," Phillips Technical Review, 20: 220-224 (Mar 1958).

Appendix A

This appendix contains the results of the reduction of data taken on four runs. The high temperature results for samples 0145 and 0151, and the high and low temperature results for sample 0288 are shown. Units of the characteristics are as follows:

resistivity	ohm-cm
Hall mobility	cm^2/volt-sec
concentration	cm^{-3}

Following the tabulated data for each sample are graphs of the characteristics versus 1000/T. The last four plots for each sample are the fits to the charge balance equation. The quantities listed on the plot are in the following units:

concentration	cm^{-3}
activation energy	ev

Sample 0145 High Temperature

Table II

TEMP	1000/T	RESISTIVITY	MOBILITY	CONCENTRATION
295.6	3.38	.116E+01	.309E+03	.174E+17
295.6	3.38	.116E+01	.310E+03	.174E+17
345.8	2.89	.112E+01	.204E+03	.272E+17
345.8	2.89	.113E+01	.213E+03	.260E+17
400.6	2.50	.123E+01	.149E+03	.340E+17
400.6	2.50	.123E+01	.151E+03	.335E+17
443.9	2.25	.139E+01	.122E+03	.368E+17
443.9	2.25	.138E+01	.121E+03	.375E+17
479.9	2.08	.153E+01	.107E+03	.379E+17
479.9	2.08	.154E+01	.107E+03	.379E+17
514.6	1.94	.171E+01	.919E+02	.396E+17
514.6	1.94	.171E+01	.890E+02	.409E+17

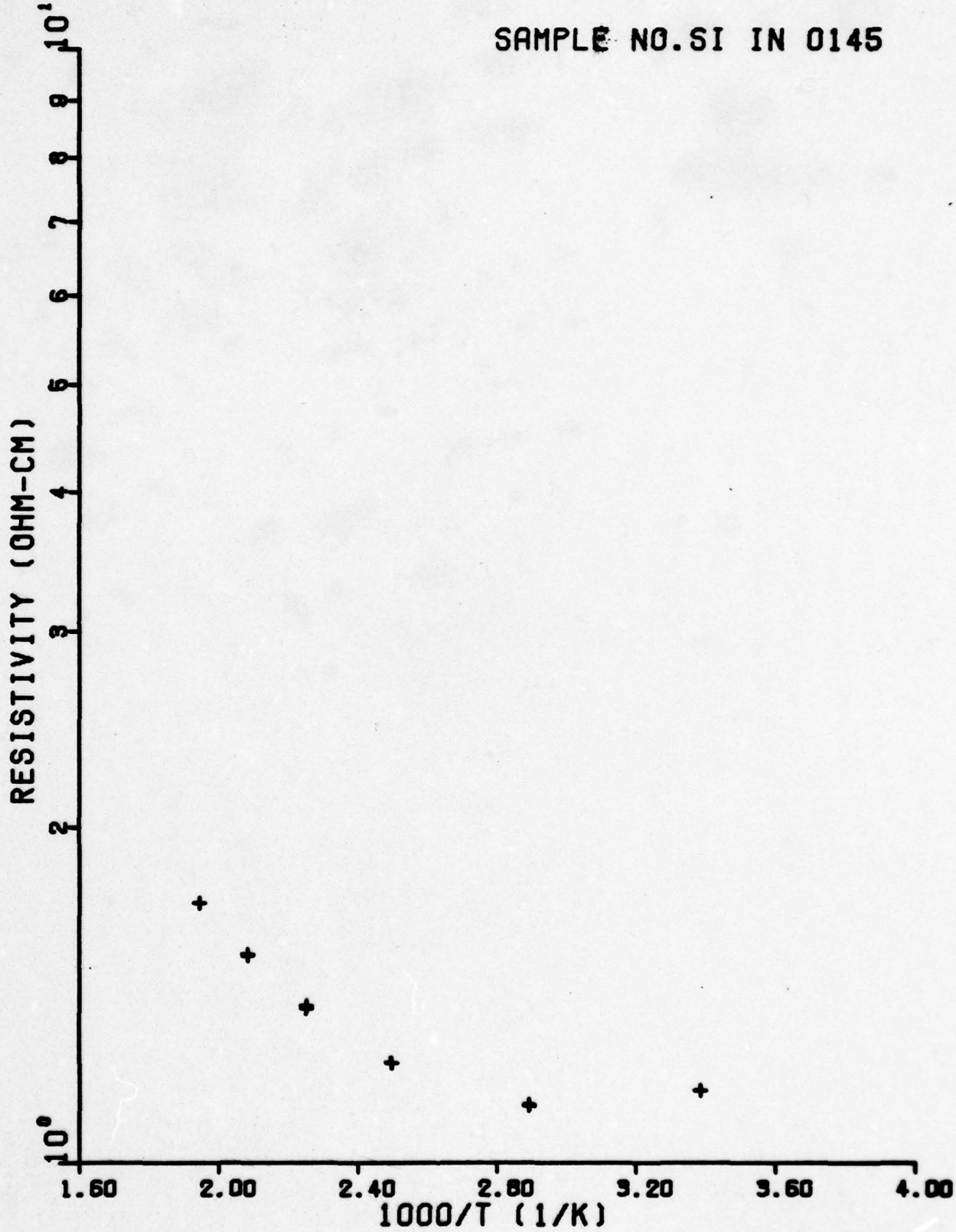

Figure A1 0145 Resistivity Versus 1000/T

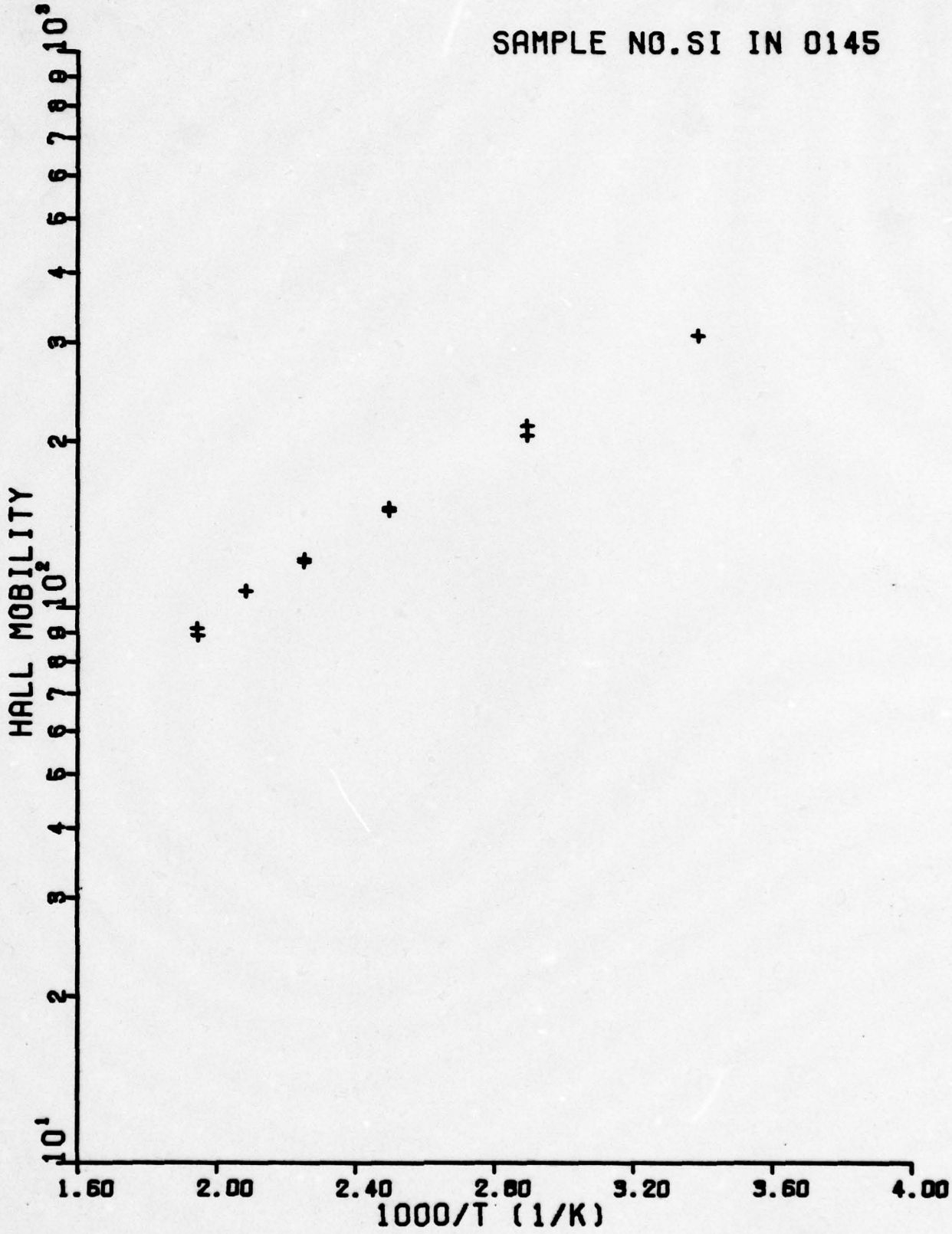

Figure A2 0145 Mobility Versus 1000/T

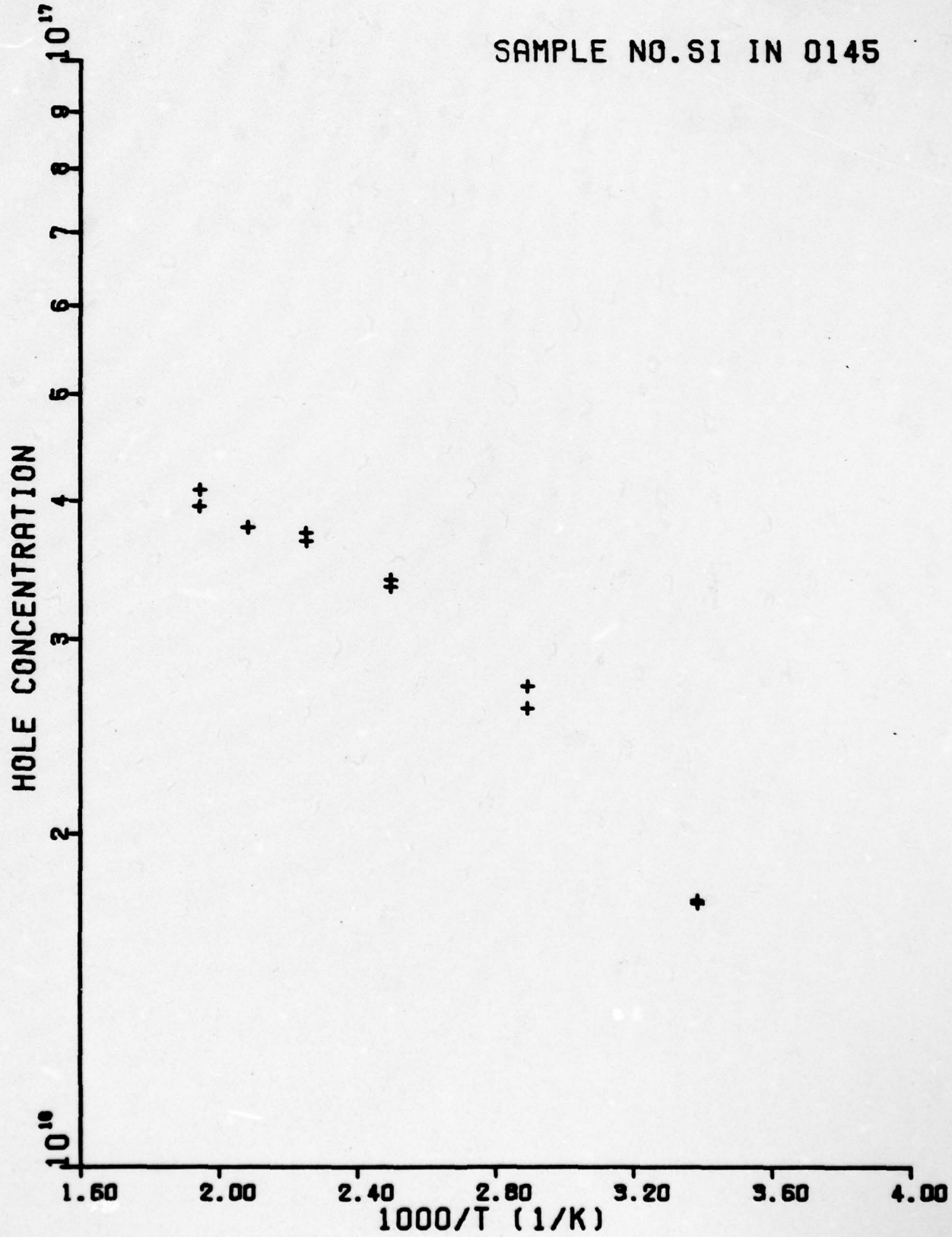

Figure A3 0145 Concentration Versus 1000/T

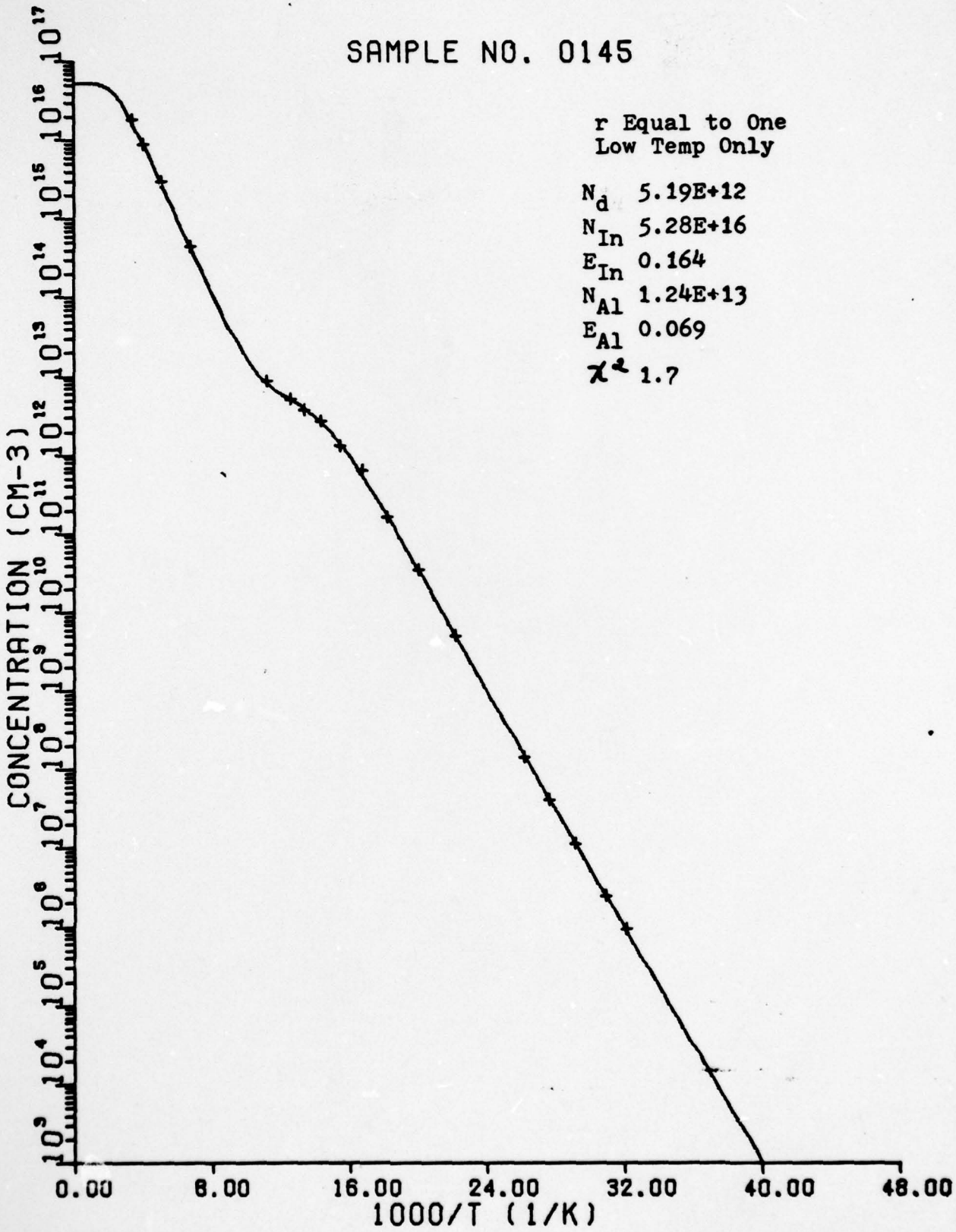

Figure A4 r = 1, Low Temperature Data

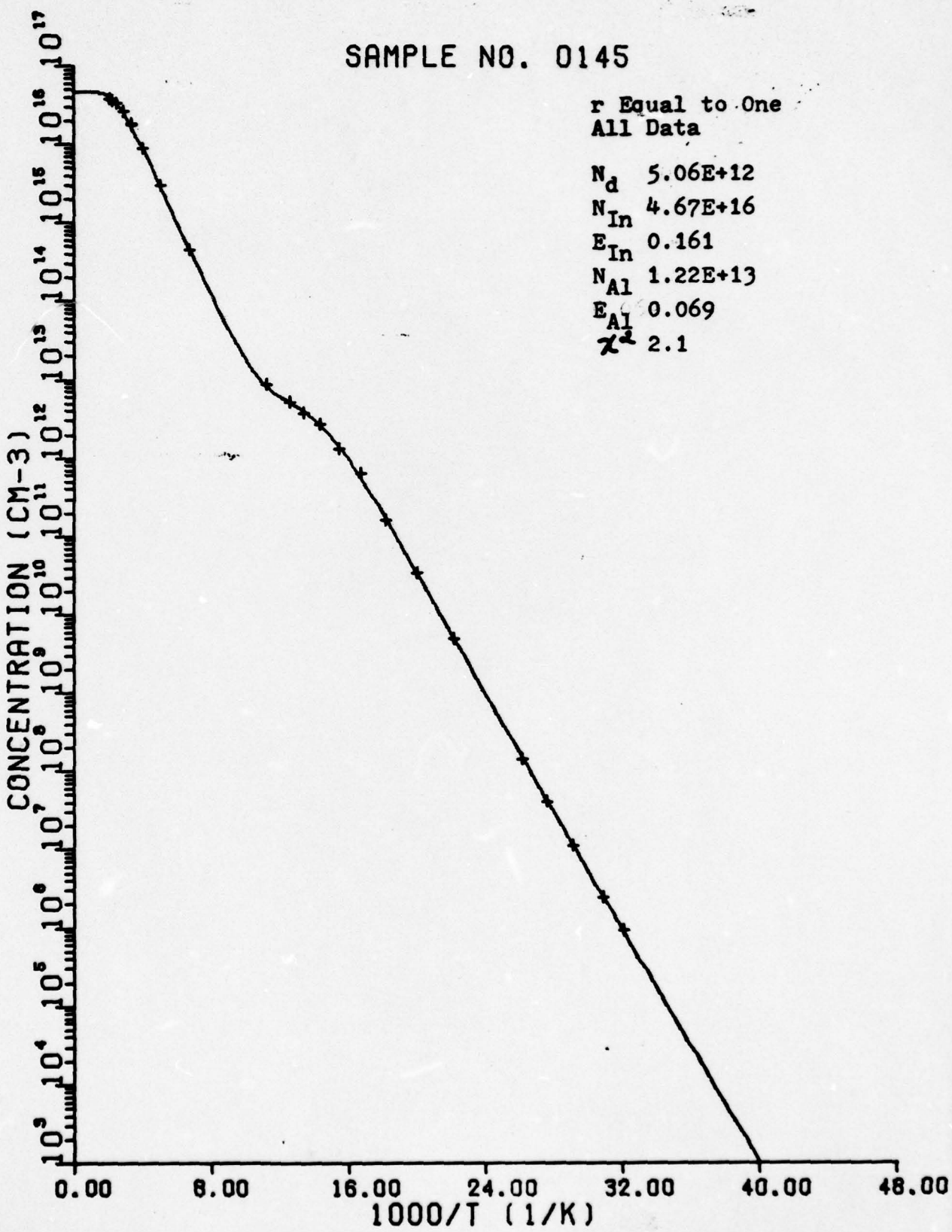

Figure A5 r = 1, All Data

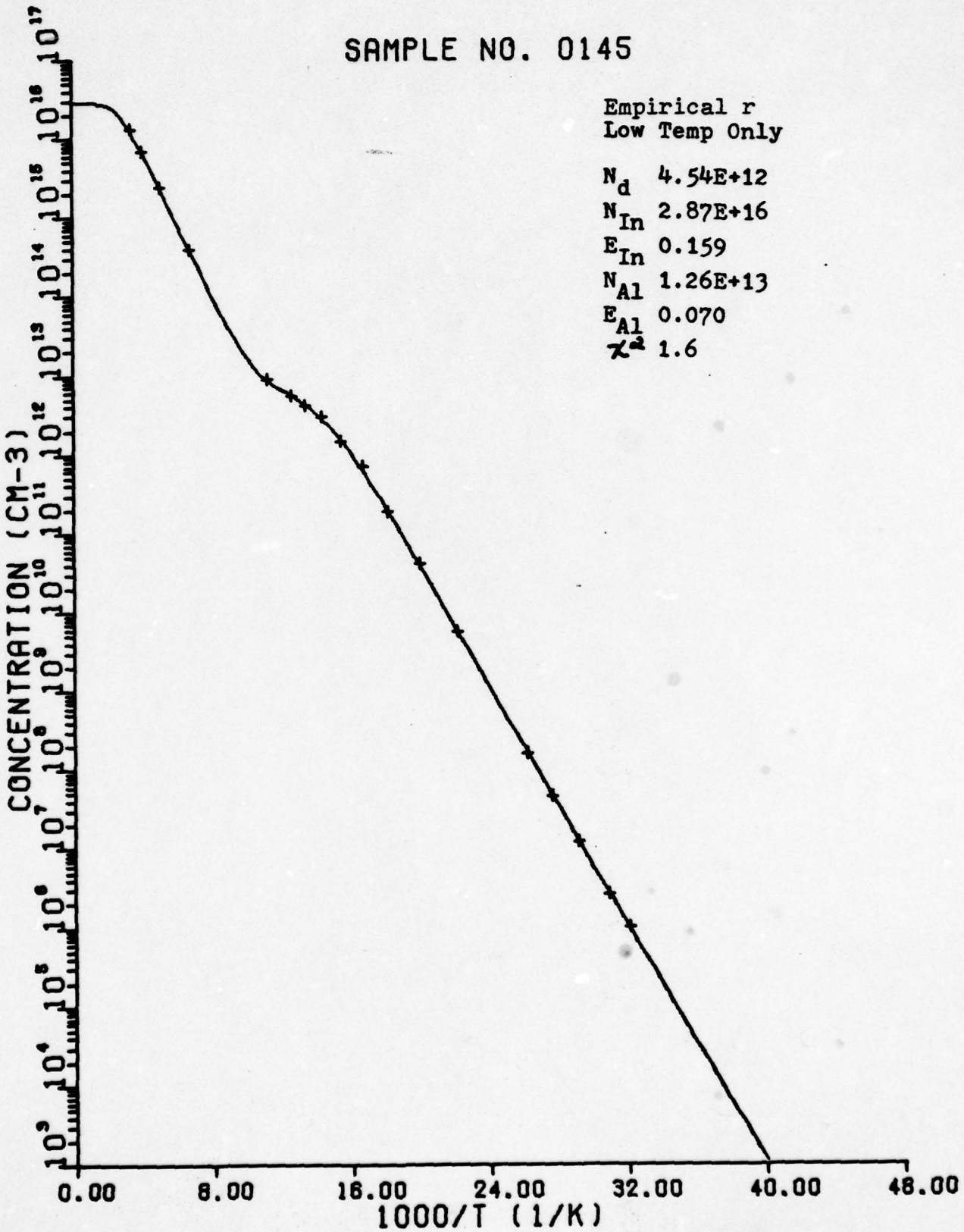

Figure A6 Empirical r, Low Data

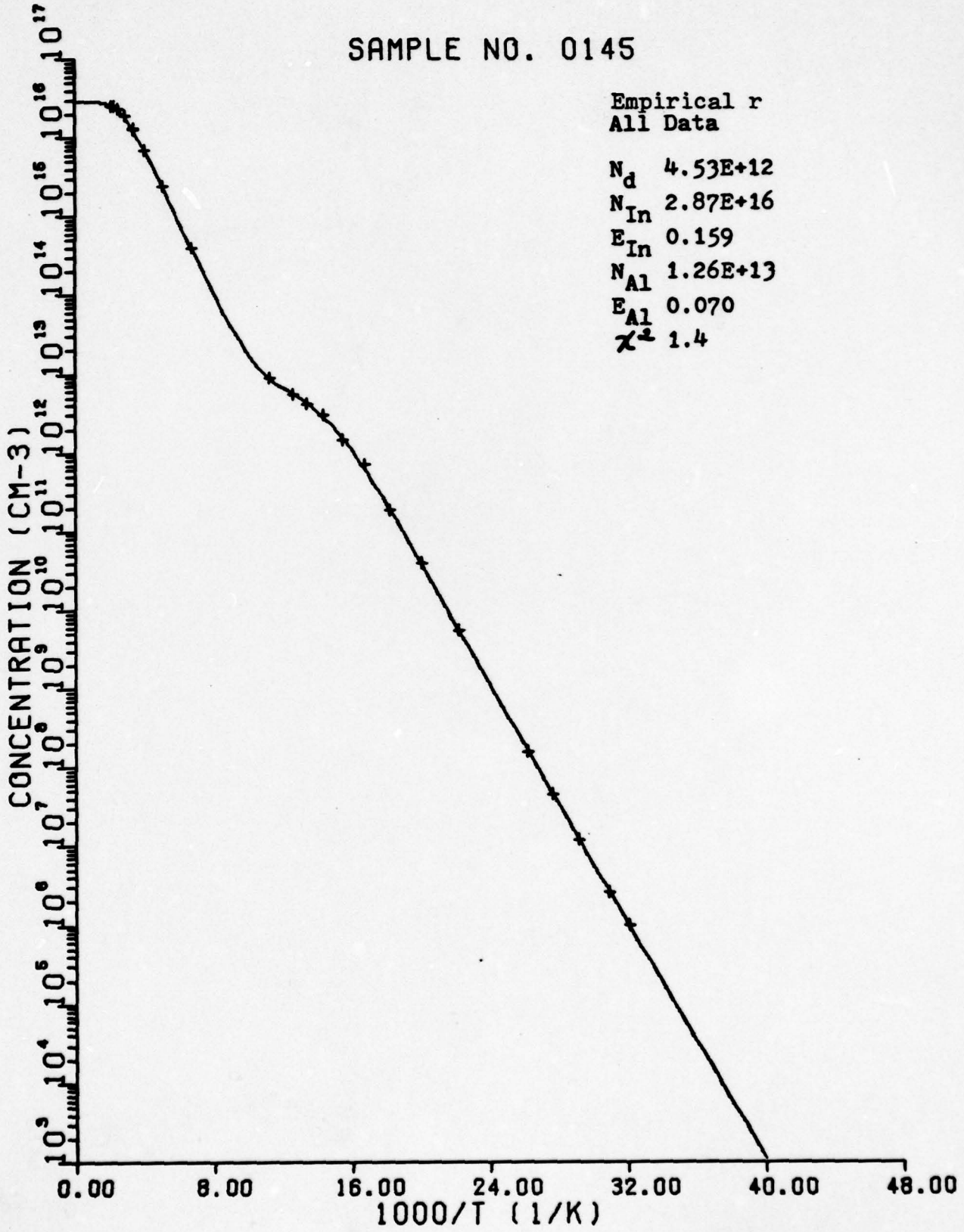

Figure A7 Empirical r, All Data

Sample 0151 High Temperature

Table III

TEMP	1000/T	RESISTIVITY	MOBILITY	CONCENTRATION
295.4	3.39	.131E+01	.320E+03	.149E+03
295.4	3.39	.131E+01	.322E+03	.148E+17
348.4	2.87	.131E+01	.241E+03	.223E+17
348.4	2.87	.131E+01	.212E+03	.225E+17
393.1	2.54	.143E+01	.163E+03	.267E+17
393.1	2.54	.143E+01	.152E+03	.268E+17
442.4	2.26	.165E+01	.128E+03	.295E+17
442.1	2.26	.165E+01	.127E+03	.298E+17
503.6	1.99	.202E+01	.956E+02	.323E+17
504.1	1.98	.203E+01	.956E+02	.322E+17
558.2	1.79	.238E+01	.738E+02	.355E+17
558.2	1.79	.238E+01	.740E+02	.354E+17
568.1	1.76	.243E+01	.687E+02	.374E+17
568.1	1.76	.243E+01	.700E+02	.367E+17

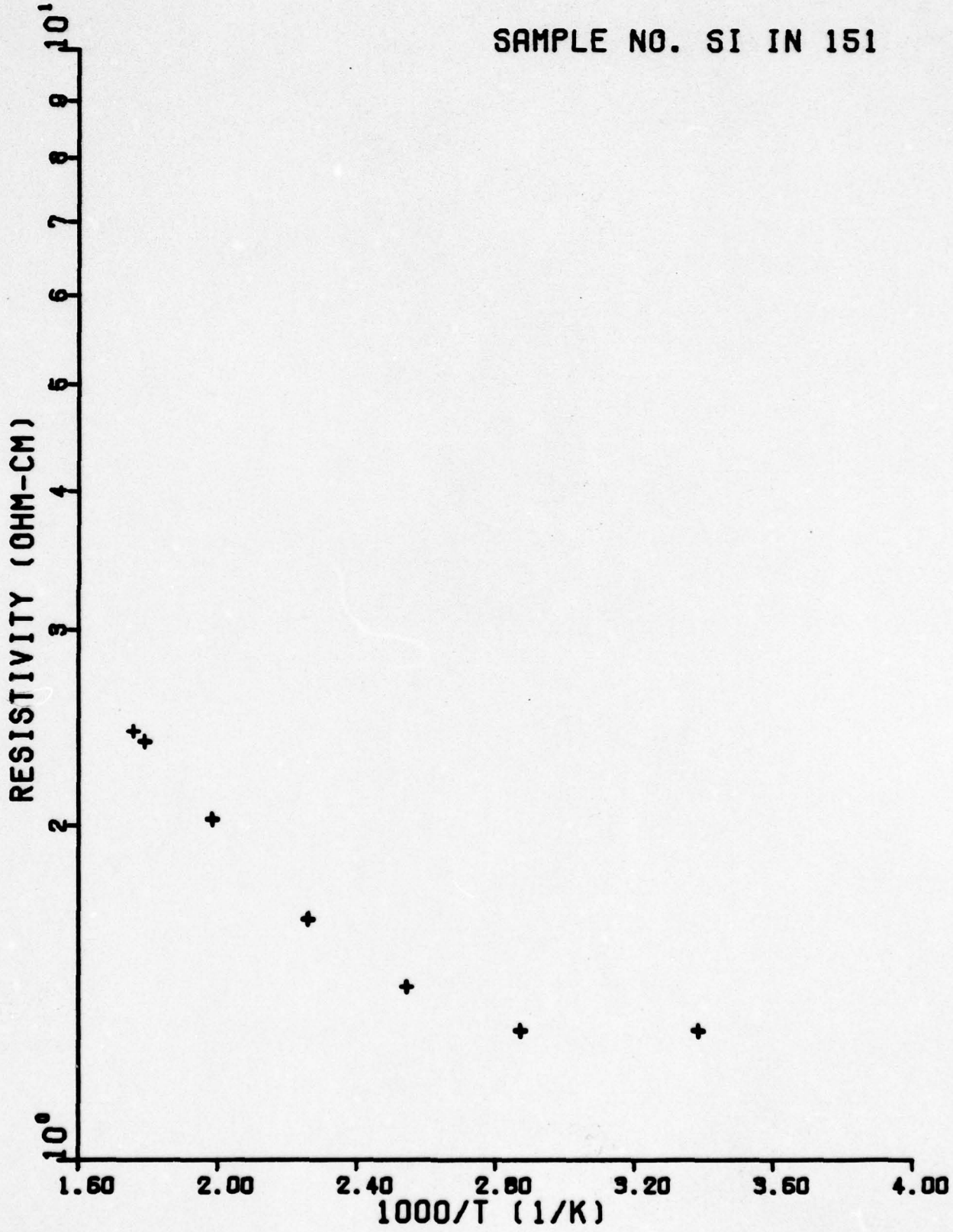

Figure A8 0151 Resistivity Versus 1000/T

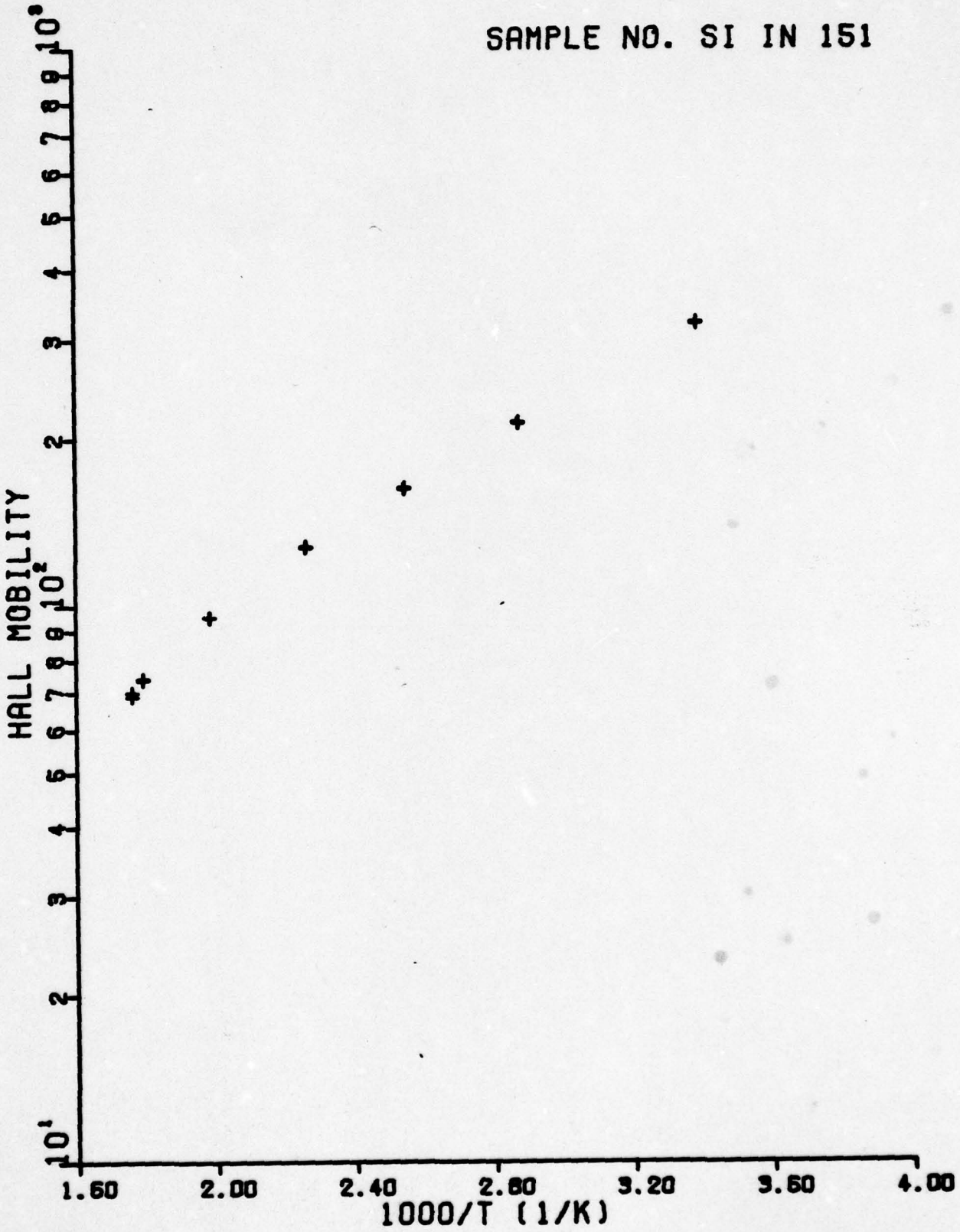

Figure A9 0151 Mobility Versus 1000/T

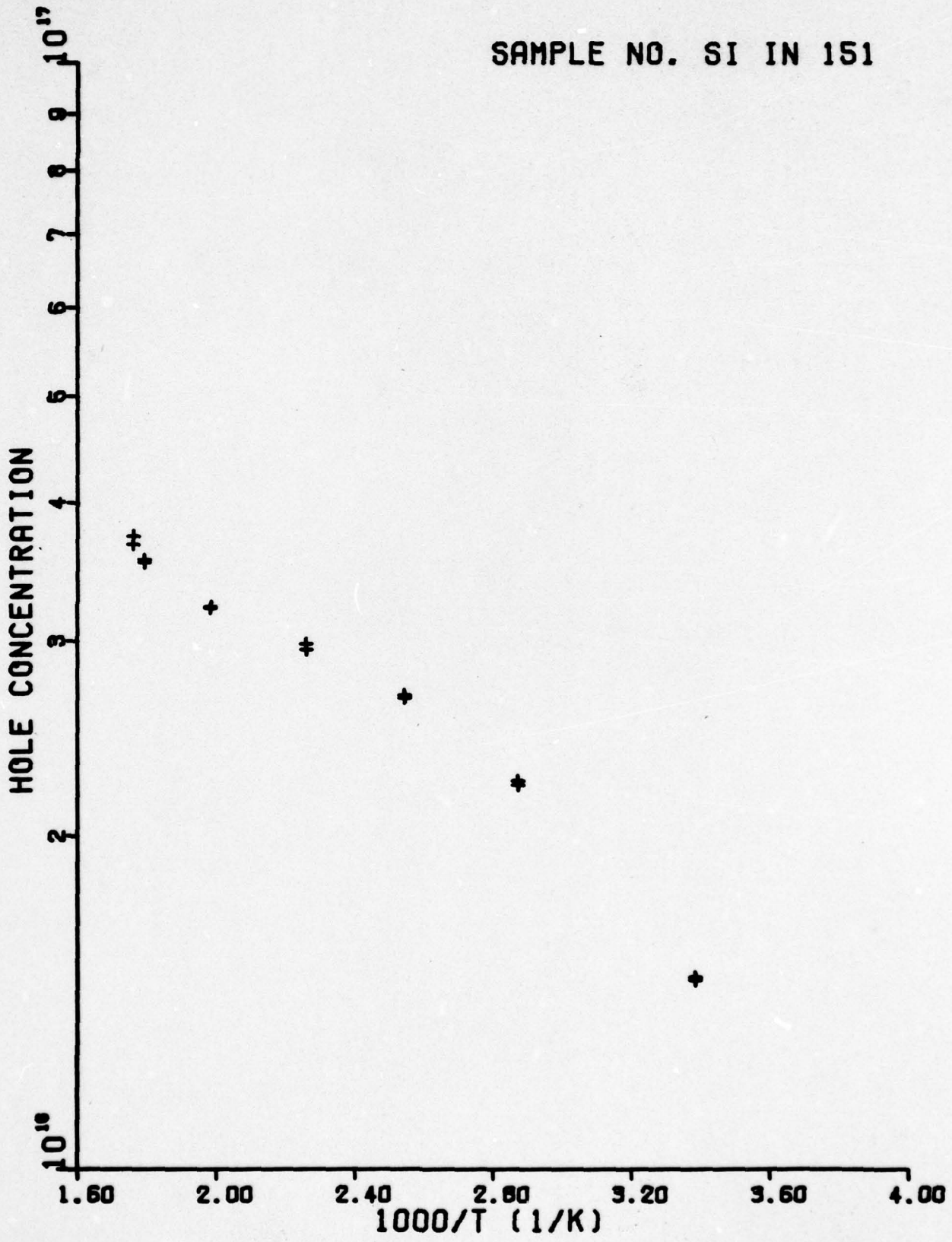

Figure A10 0151 Concentration Versus 1000/T

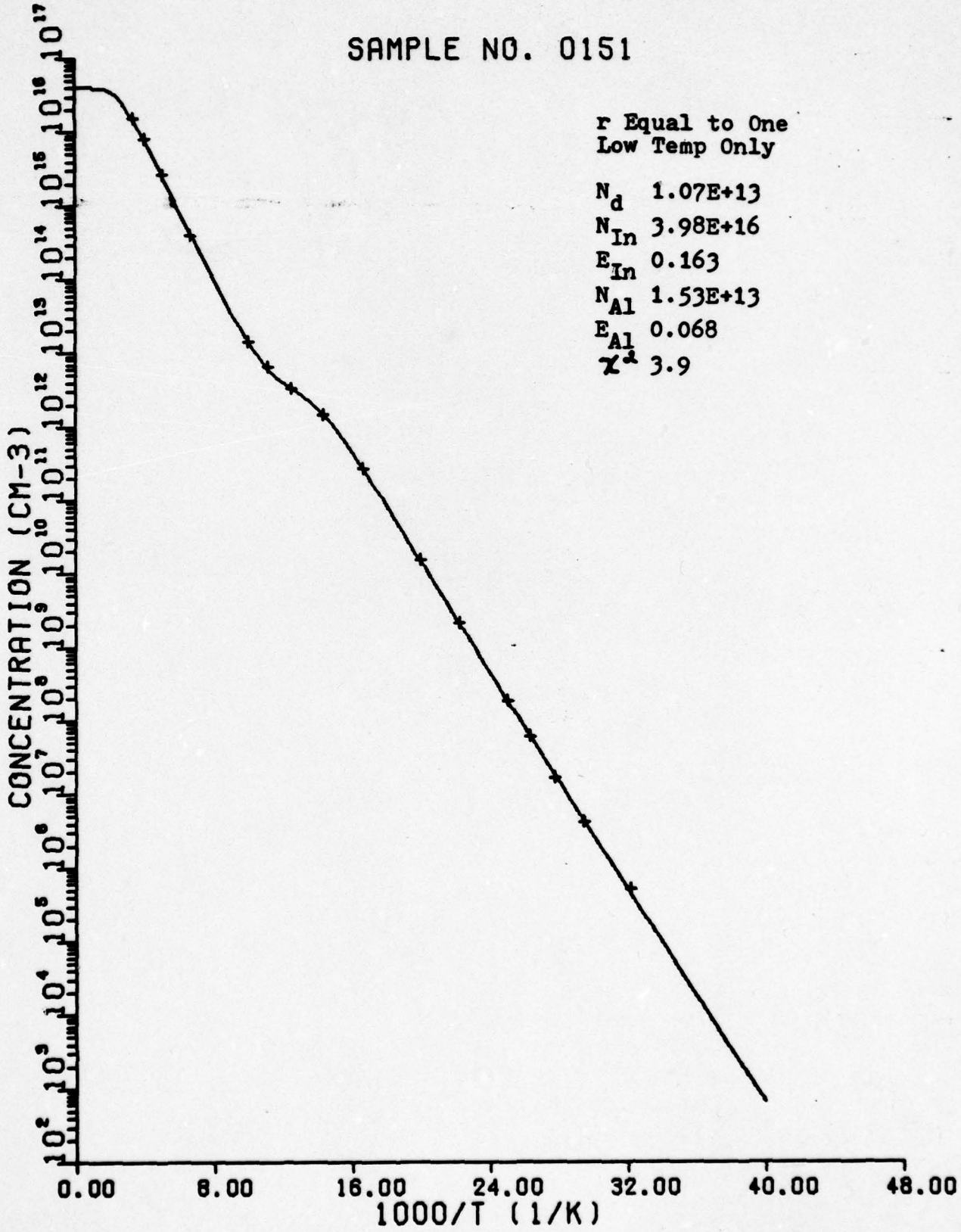

Figure A11 Low Data, r = 1

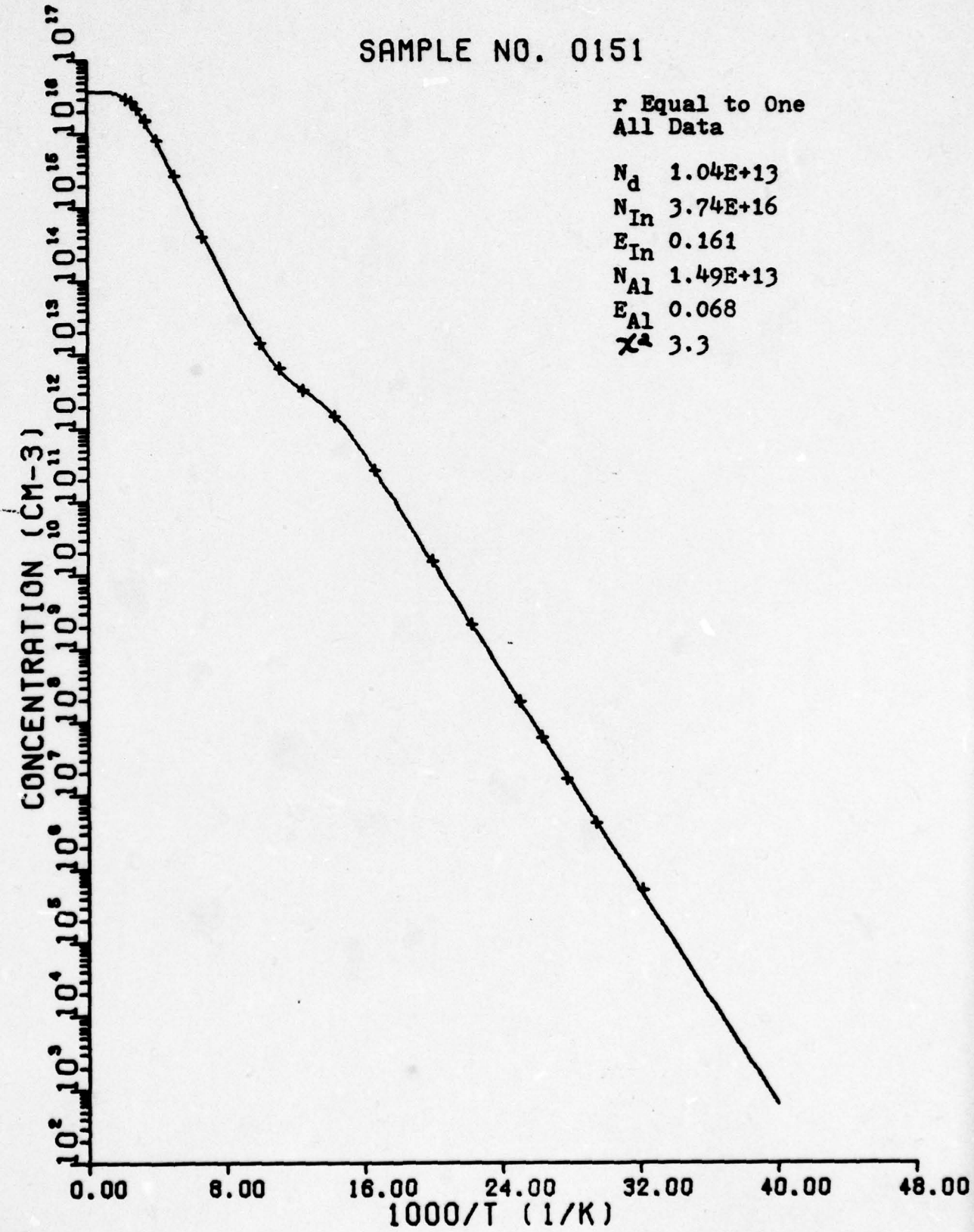

Figure A12 All Data, r = 1

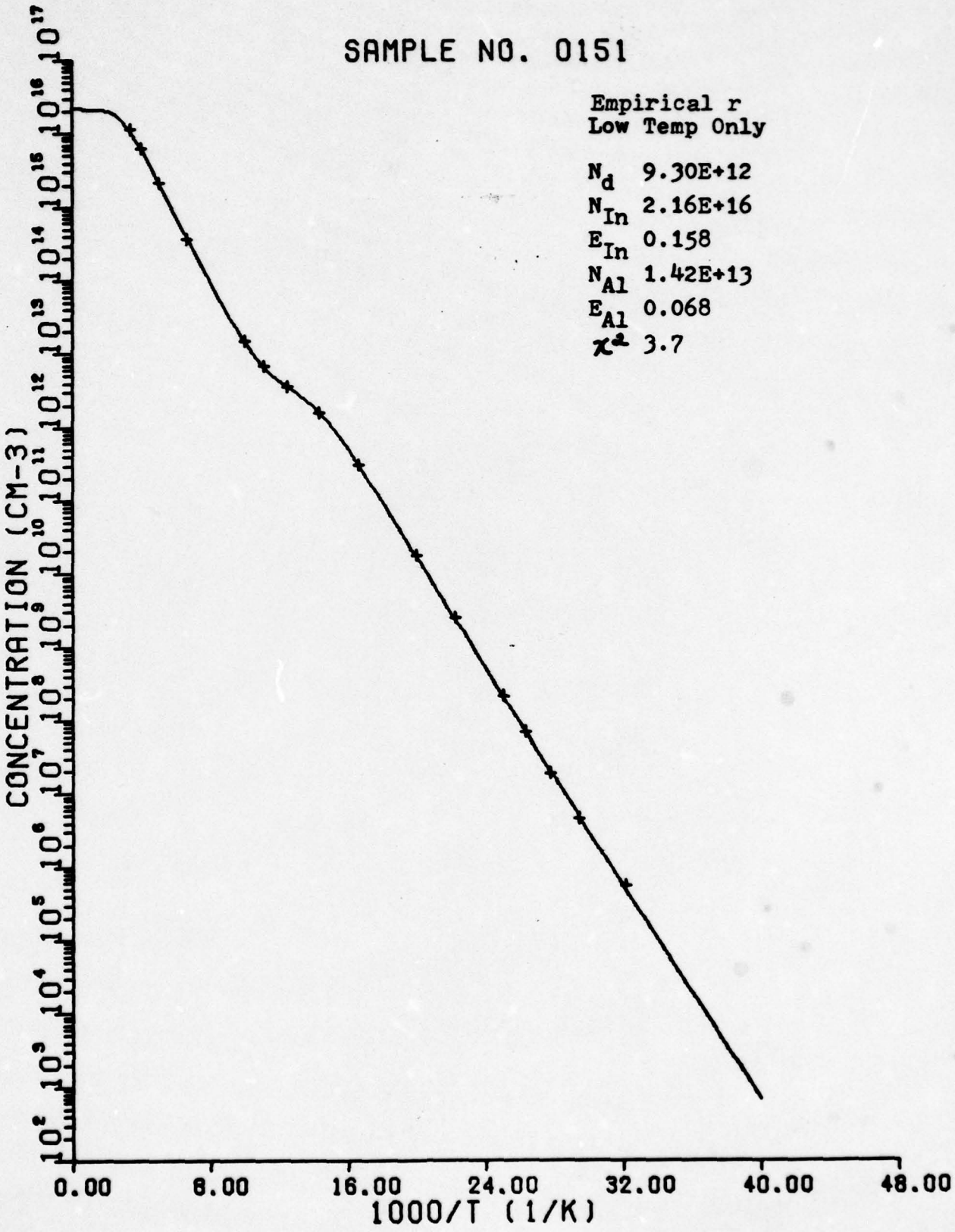

Figure A13 Low Data, Empirical

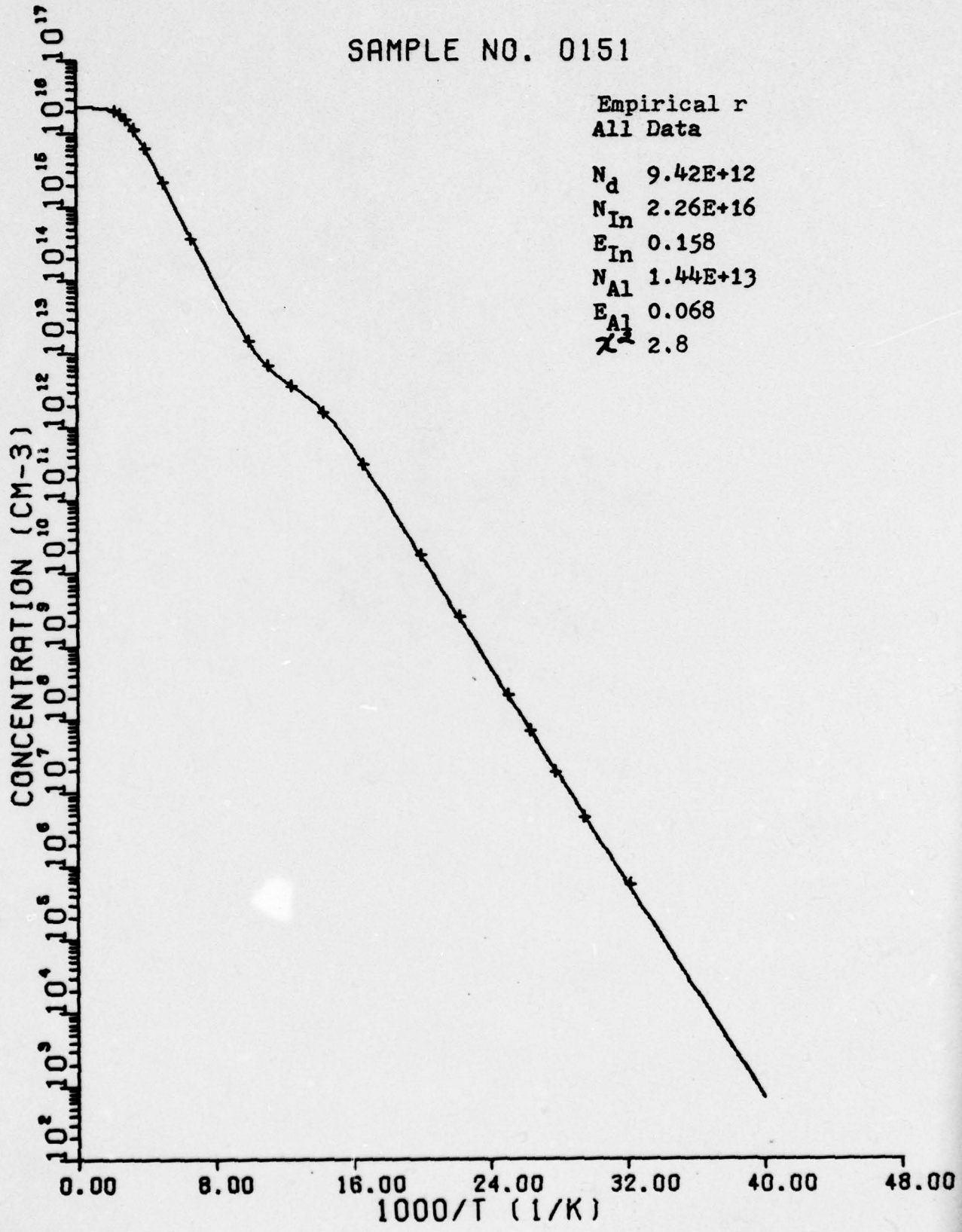

Figure A14 All Data, Empirical r

Sample 0288 High Temperature

Table IV

TEMP	1000/T	RESISTIVITY	MOBILITY	CONCENTRATION
294.9	3.39	.351E+00	.242E+03	.736E+17
294.9	3.39	.352E+00	.242E+03	.735E+17
318.9	3.14	.319E+00	.204E+03	.959E+17
318.9	3.14	.317E+00	.202E+03	.975E+17
366.7	2.73	.280E+00	.151E+03	.148E+18
366.7	2.73	.279E+00	.147E+03	.153E+18
410.4	2.44	.265E+00	.117E+03	.202E+18
410.4	2.44	.265E+00	.117E+03	.201E+18
477.1	2.10	.266E+00	.871E+02	.269E+18
477.1	2.10	.266E+00	.883E+02	.266E+18
524.5	1.91	.277E+00	.722E+02	.312E+18
525.2	1.90	.278E+00	.720E+02	.312E+18
563.2	1.78	.292E+00	.644E+02	.332E+18
563.2	1.78	.292E+00	.659E+02	.324E+18
611.1	1.64	.315E+00	.554E+02	.358E+18
609.6	1.64	.313E+00	.547E+02	.364E+18
664.4	1.51	.340E+00	.459E+02	.400E+18
664.4	1.51	.340E+00	.468E+02	.394E+18
688.8	1.45	.351E+00	.385E+02	.463E+18
688.8	1.45	.351E+00	.363E+02	.491E+18
746.3	1.34	.338E+00	.220E+02	.840E+18
746.3	1.34	.335E+00	.213E+02	.876E+18

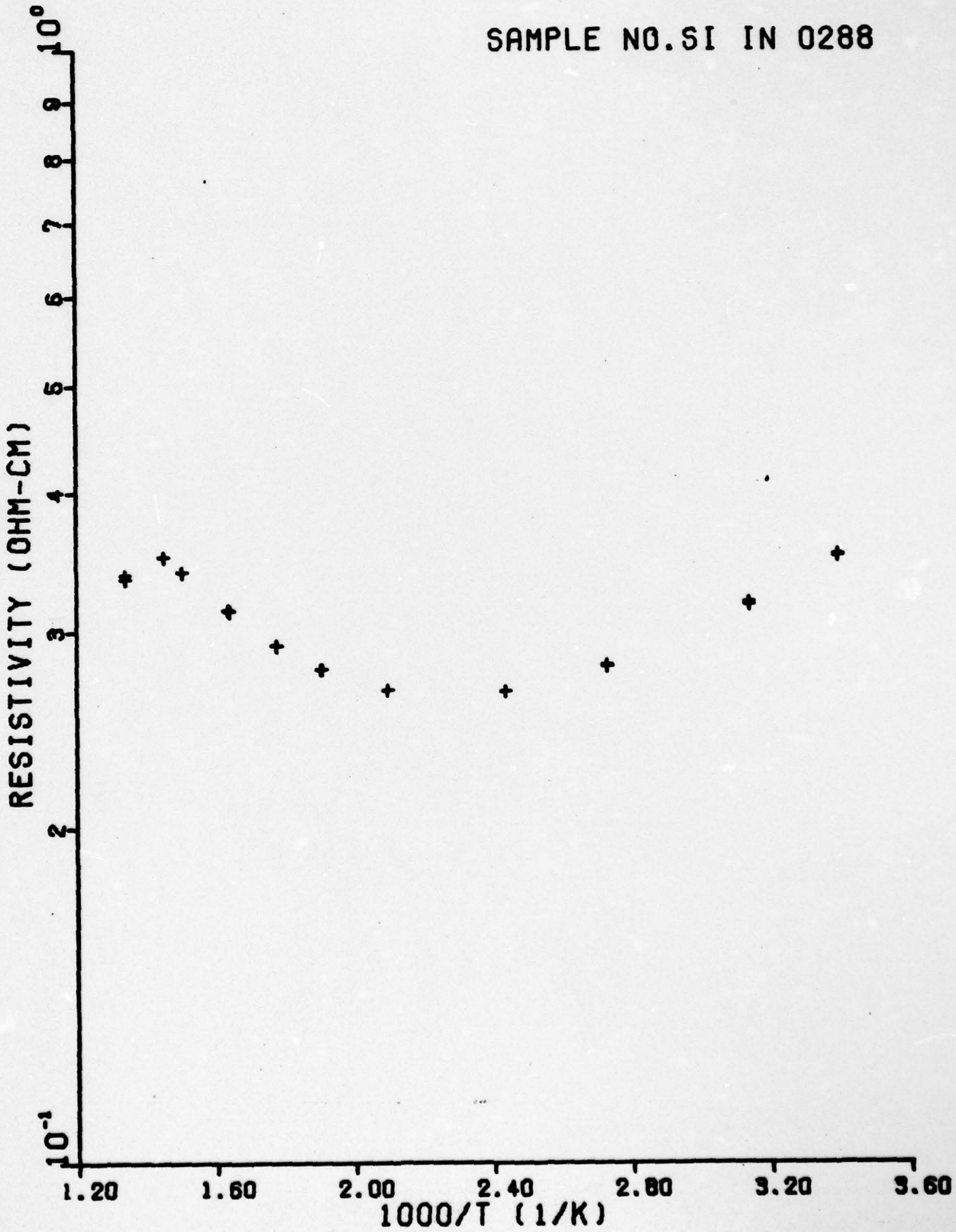

Figure A15 0288 Resistivity Versus 1000/T (High)

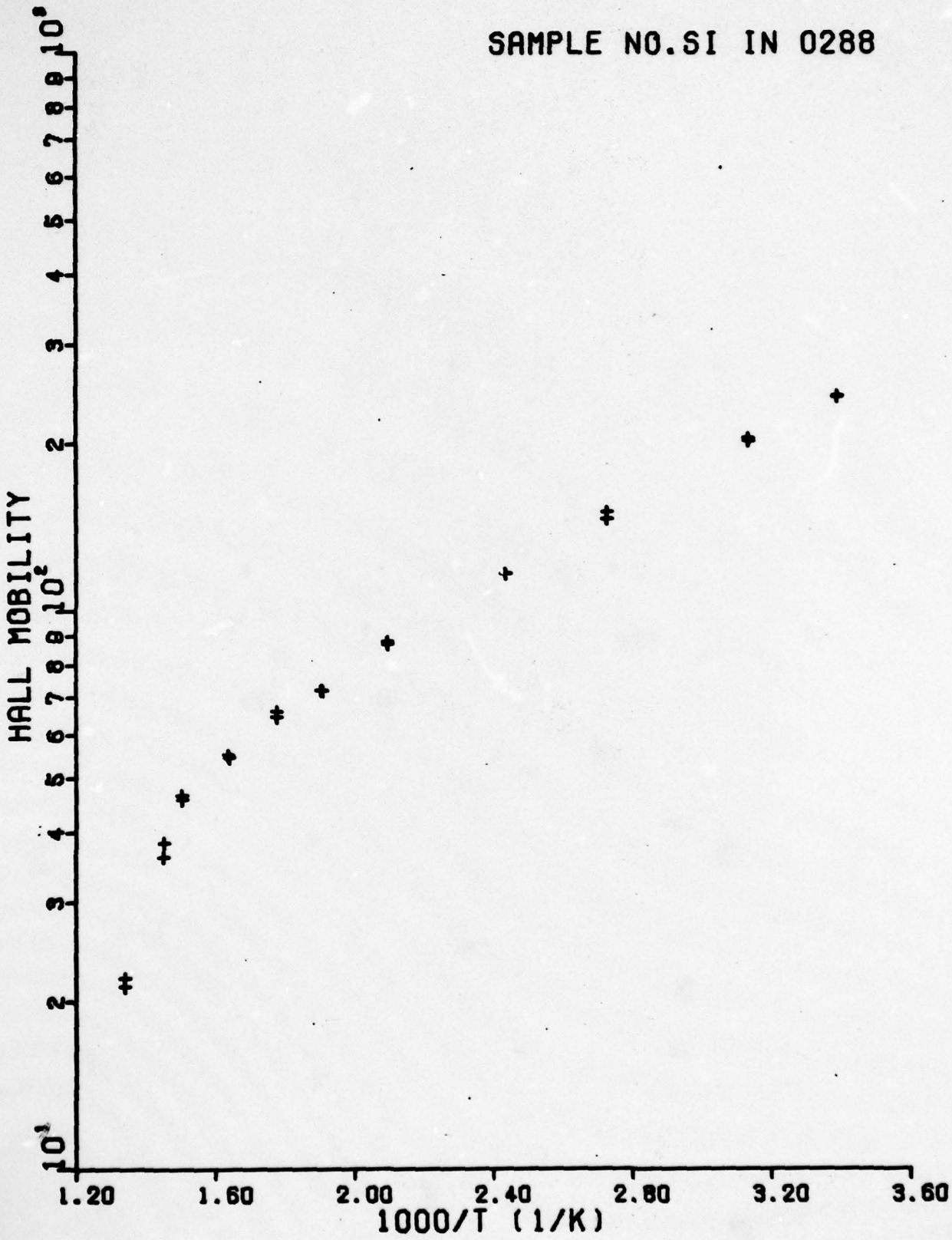

Figure A16 0288 Mobility Versus 1000/T (High)

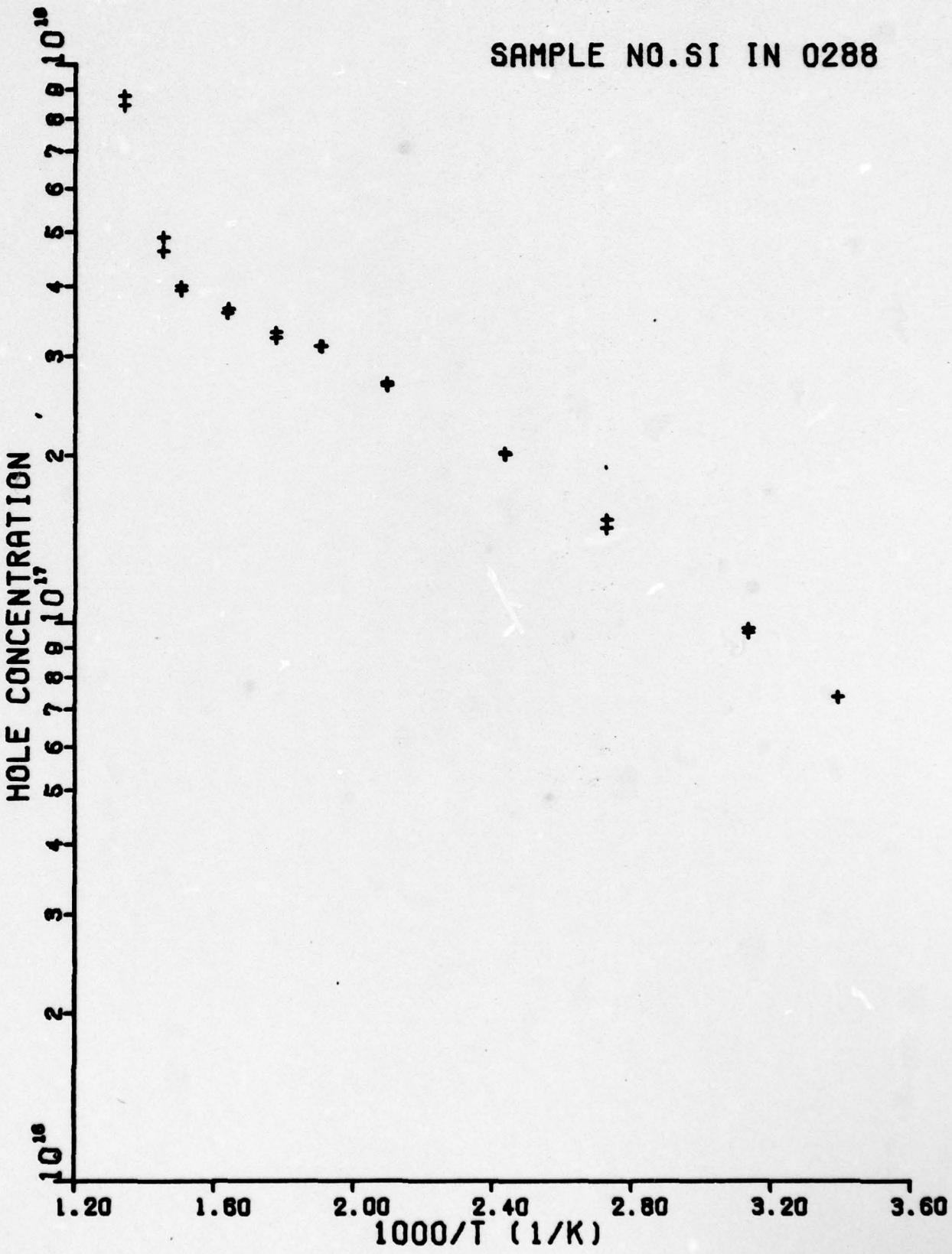

Figure A17 0288 Concentration Versus 1000/T (High)

Sample 0288 Low Temperature

Table V

TEMP	1000/T	RESISTIVITY	MOBILITY	CONCENTRATION
55.2	13.11	.115E+09	.287E+04	.189E+08
61.5	15.26	.599E+07	.274E+04	.381E+09
64.9	15.40	.138E+07	.263E+04	.172E+10
74.9	13.35	.360E+05	.232E+04	.749E+11
80.0	12.50	.779E+04	.219E+04	.365E+12
90.0	11.11	.704E+03	.198E+04	.448E+13
105.0	3.52	.625E+02	.185E+04	.539E+14
120.0	8.33	.148E+02	.169E+04	.249E+15
150.0	6.67	.301E+01	.126E+04	.165E+16
200.0	5.00	.875E+00	.655E+03	.109E+17
250.0	4.00	.481E+00	.386E+03	.337E+17
300.0	3.33	.341E+00	.243E+03	.754E+17
360.1	2.78	.281E+00	.165E+03	.135E+18

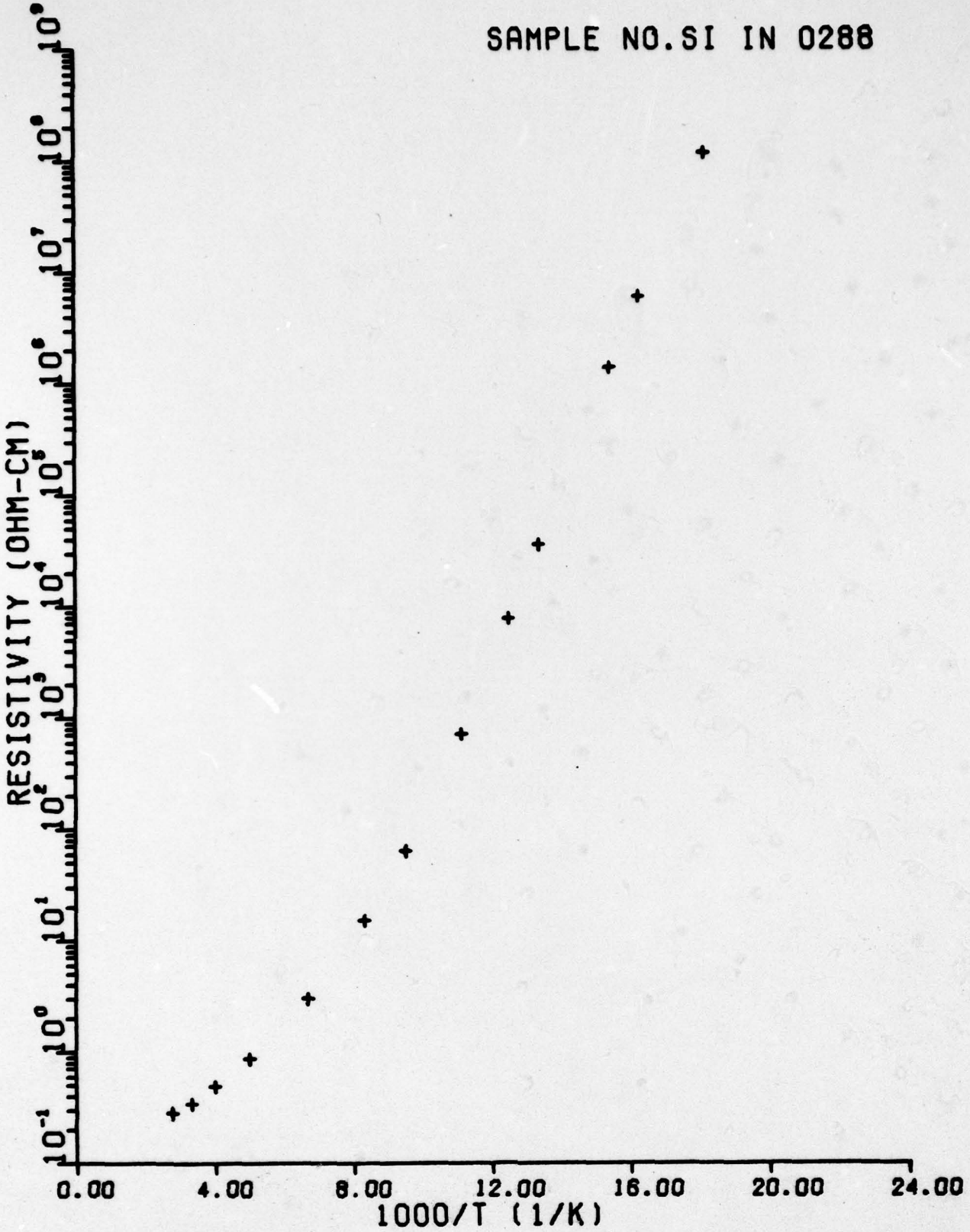

Figure A20 0288 Resistivity Versus 1000/T (Low)

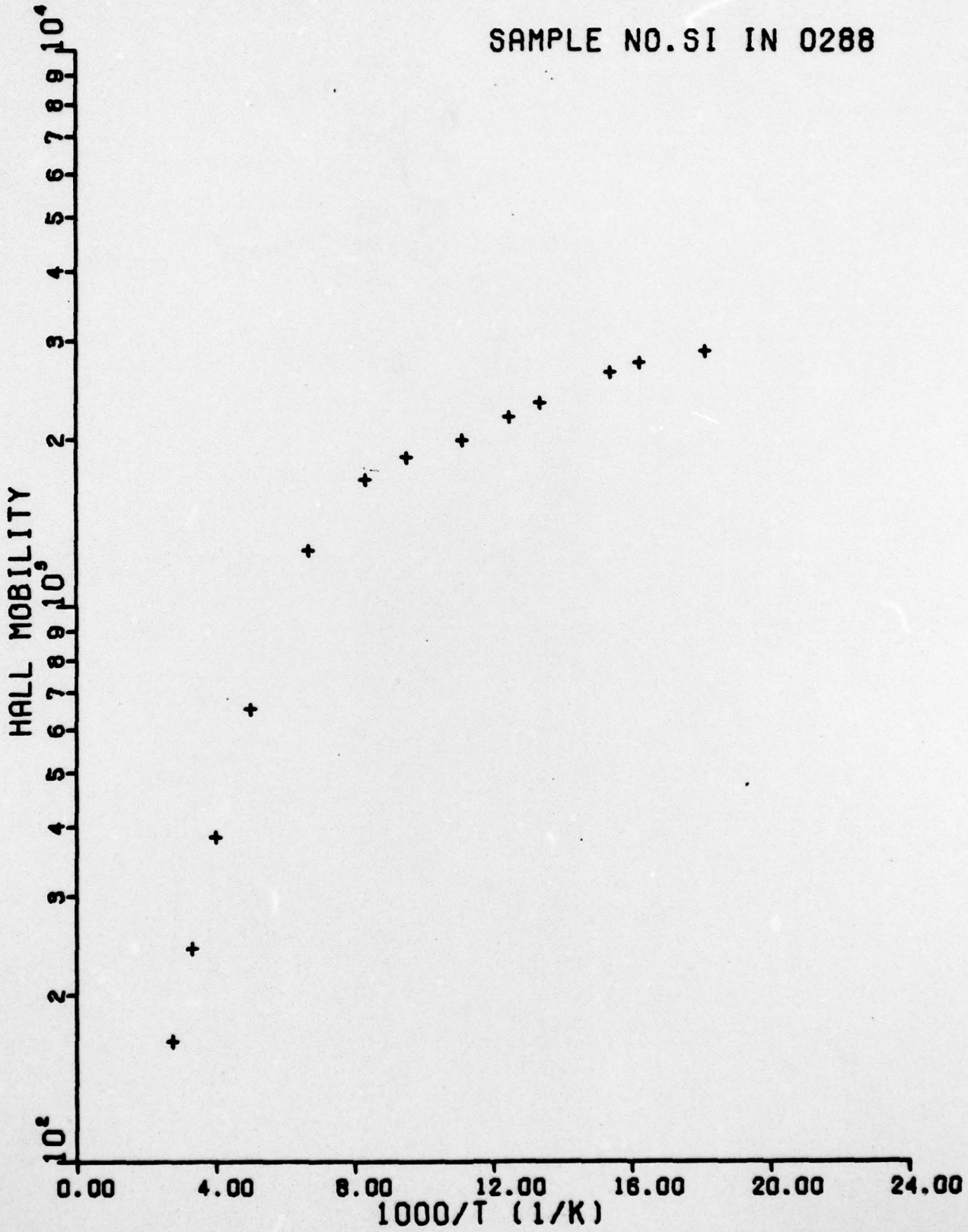

Figure A19 0288 Mobility Versus 1000/T (Low)

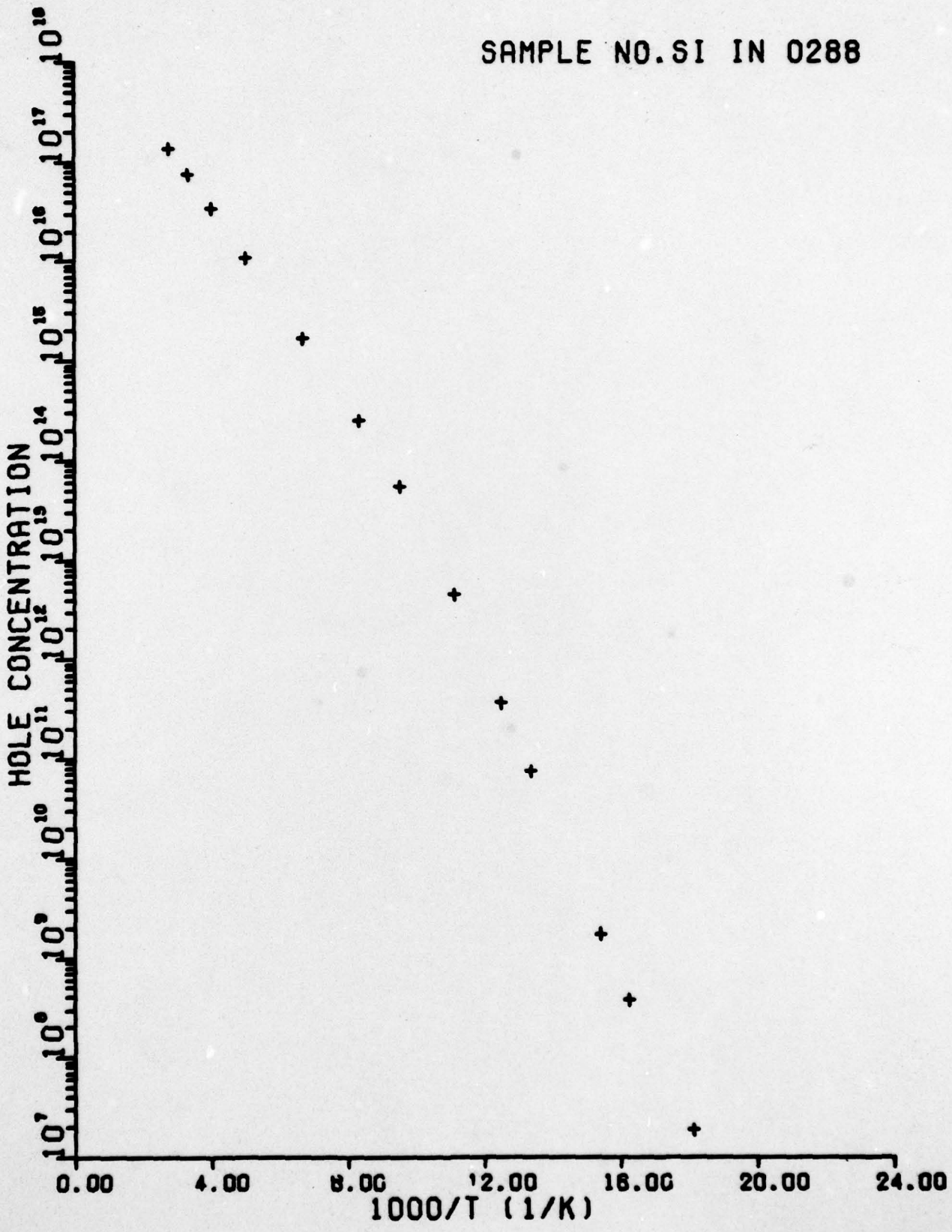

Figure A20 0288 Concentration Versus 1000/T (Low)

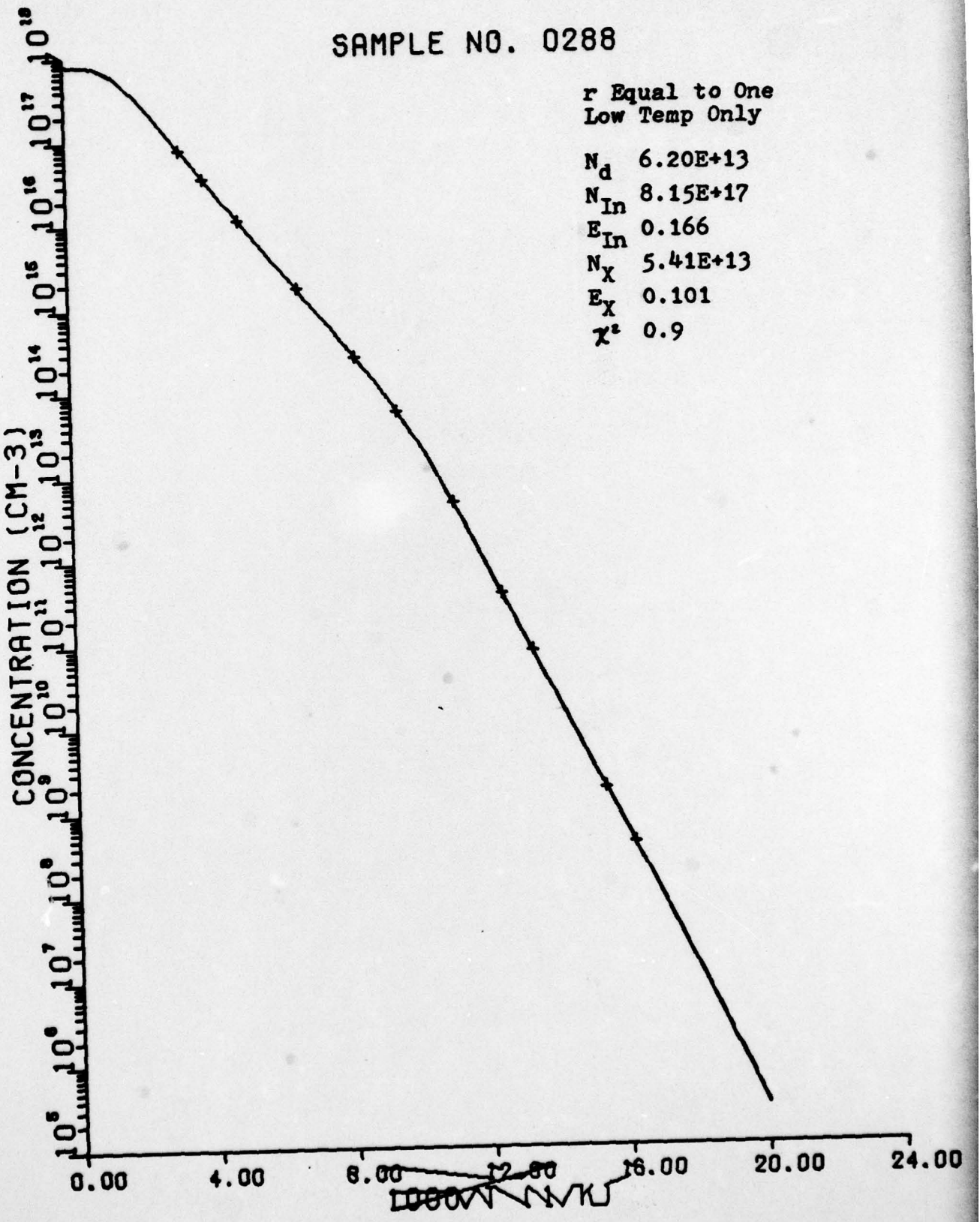

Figure A21 Low Data, r = 1

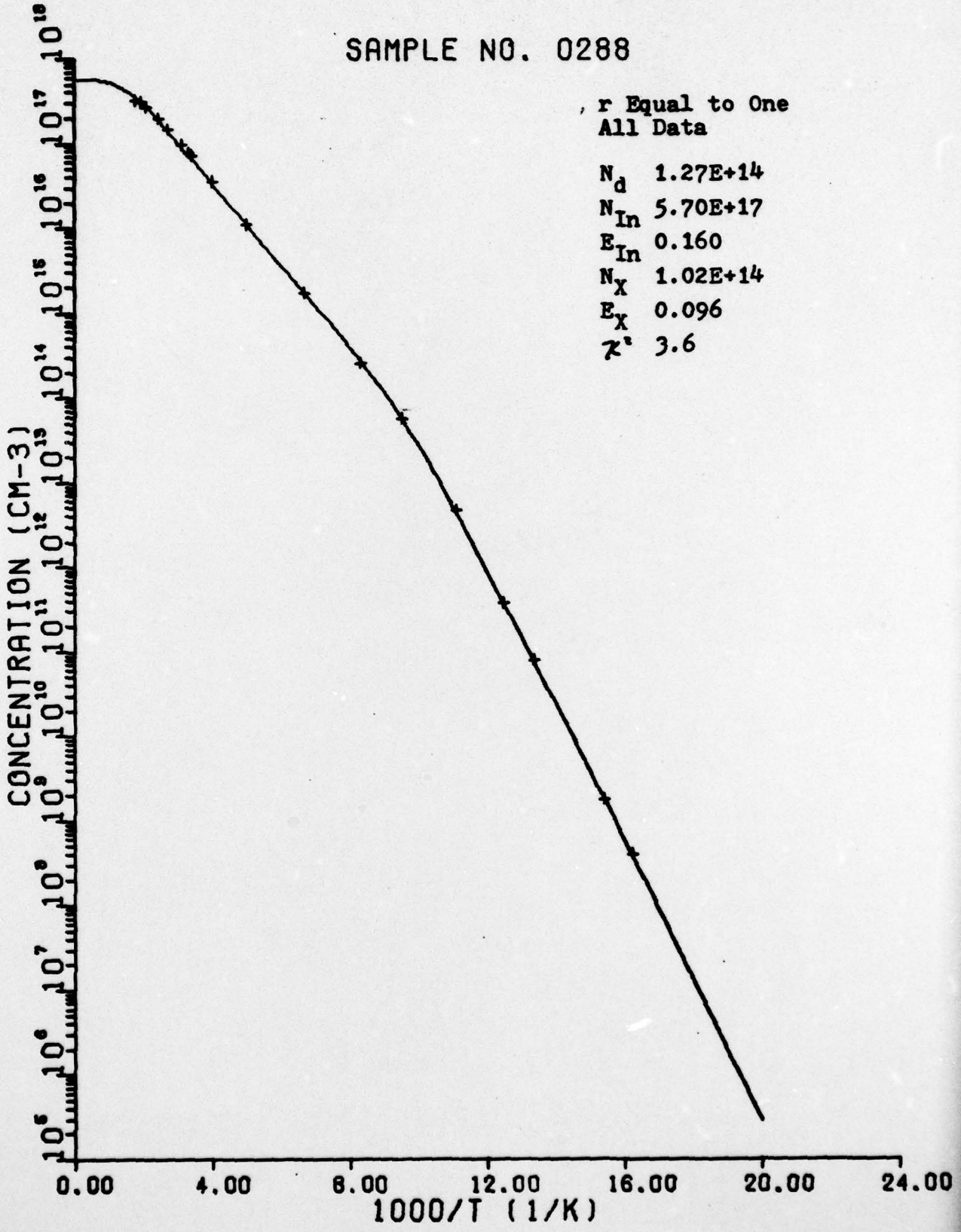

Figure A22 All Data, r = 1

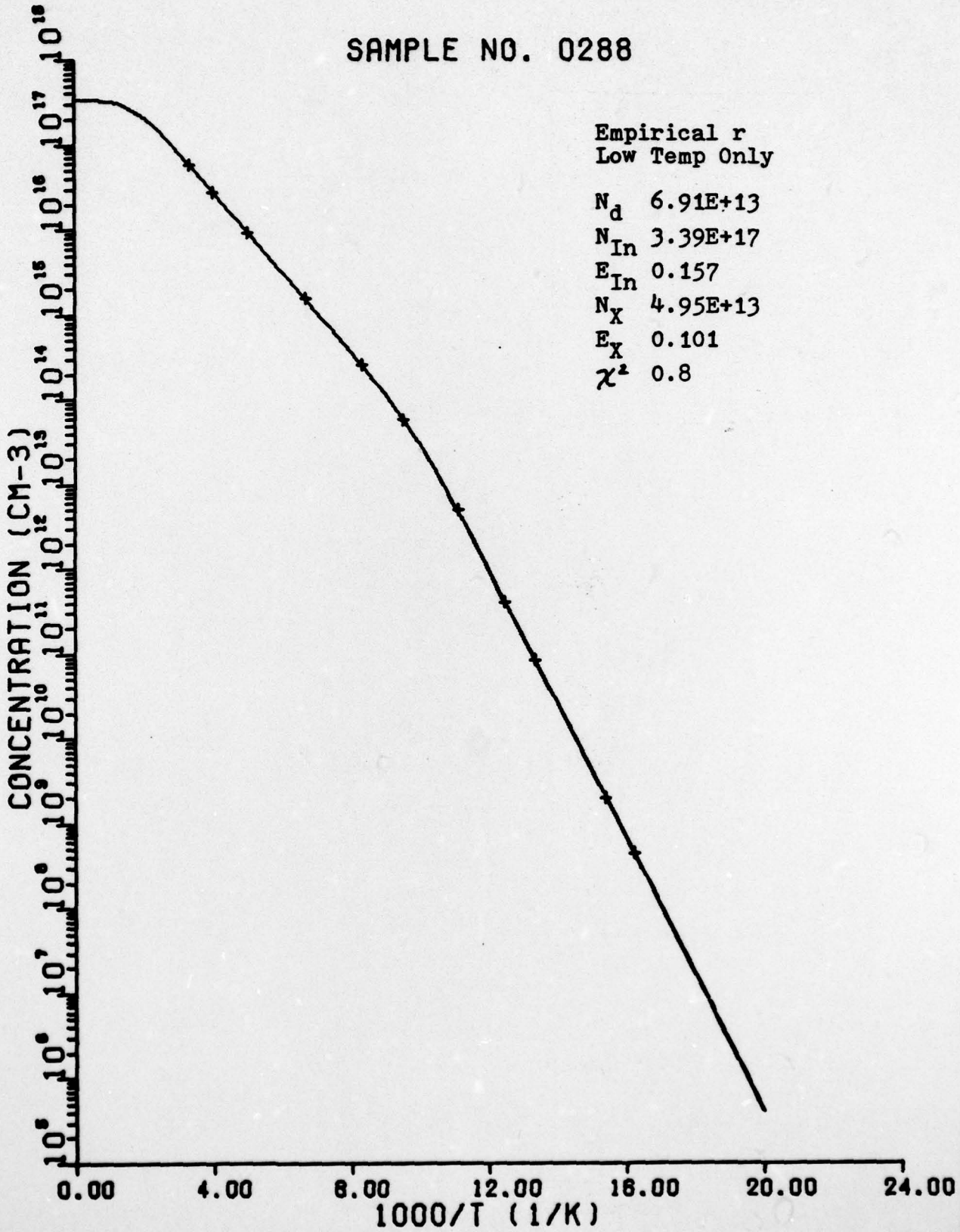

Figure A23 Low Data, Empirical r

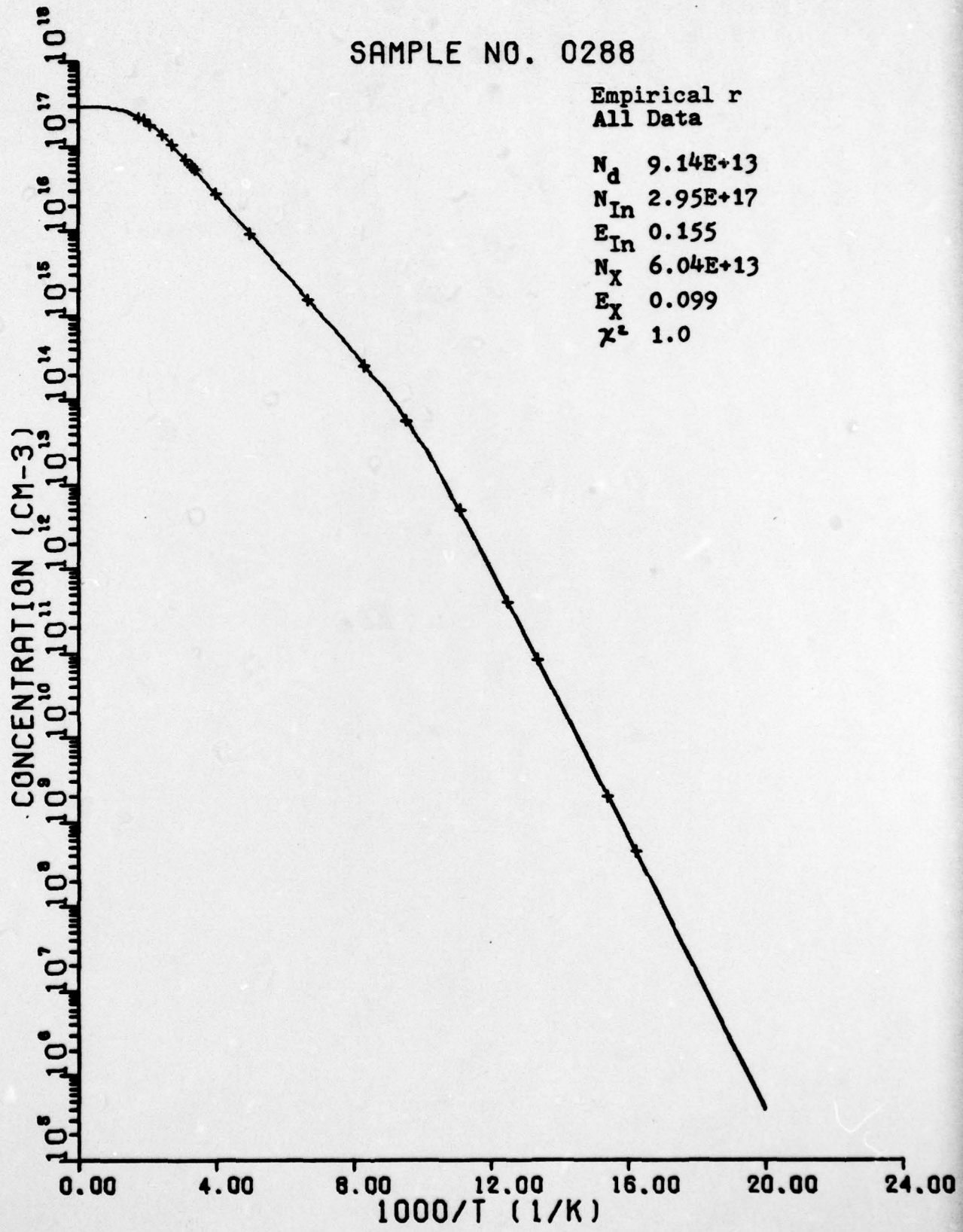

Figure A24 All Data, Empirical r

Appendix B

This appendix shows the derivation of the slope of ln p versus 1/T in the extrinsic region. In general, for low temperature, Eq (18) applies:

$$p = \frac{(N_a - N_d)}{N_d} \frac{N_F}{g} \exp\frac{-E_a}{kT} \tag{B1}$$

Taking the natural logarithm of each side:

$$\ln p = \ln\left(\frac{N_a - N_d}{N_d\, g}\right) + \ln N_F - \frac{E_a}{kT} \tag{B2}$$

Only the last two terms are temperature dependent. N_F contains the terms $\left[m_h^*(T)\right]^{3/2}$ and $T^{3/2}$, so Eq (B2) may be written as:

$$\ln p = \ln C_1 + \ln C_2 + \frac{3}{2} \ln m_h^* T - \frac{E_a}{kT} \tag{B3}$$

where

$$C_1 = \frac{N_a - N_d}{N_a\, g} \tag{B4}$$

$$C_2 = \frac{2(2\pi k)^{3/2}}{h^3} \tag{B5}$$

Letting X = 1/T and taking the derivative with respect to X:

$$\frac{d(\ln p)}{dx} = \frac{-3}{2x} - \frac{E_a}{k} + \frac{3}{2} d \frac{[m_h^*(1/x)]}{dx} \quad \text{(B6)}$$

Since the variation of effective mass with respect to inverse temperature is small compared to the other two terms:

$$\Delta \ln p = \left| \frac{3}{2} T + \frac{E_a}{k} \right| \Delta \left(1/T \right) \quad \text{(B7)}$$

For the special case that $N = N_a$, Eq (19) applies:

$$p = \left(\frac{N_a N_v}{g} \right)^{1/2} \exp \frac{-E_a}{2kT} \quad \text{(B8)}$$

Proceeding in a manner similar to the above, Eq (B9) is obtained:

$$\Delta \ln p = \left| \frac{3}{4} T + \frac{E_a}{2k} \right| \Delta \left(1/T \right) \quad \text{(B9)}$$

At low temperatures such that E_a is much greater than kT, the temperature term in Eq (B7) and Eq (B9) may be ignored and the slopes are approximately E_a/k and $E_a/2k$ respectively.

Appendix C

This appendix derives the relative error in free carrier concentration due to temperature error for the region characterized by the $E_a/2$ slope. The concentration in this region is given by Eq (19):

$$p = \left(\frac{N_a N_F}{g}\right)^{1/2} \exp\frac{-E_a}{2kT} \tag{C1}$$

where

$$N_F = \frac{2(2\pi m^* kT)^{3/2}}{h^3} \tag{C2}$$

thus,

$$p = \left(\frac{N_a 2}{g}\right)^{1/2} \left(\frac{2\pi m^* k}{h^3}\right)^{3/4} T^{3/4} \exp\frac{-E_a}{2kT} \tag{C3}$$

Taking the derivative with respect to T:

$$\frac{dp}{dT} = \left(\frac{N_a 2}{g}\right)^{1/2} \left(\frac{2\pi m^* k}{h^3}\right)^{3/4} \left[\frac{3}{4}T^{-1/4} \exp\frac{-E_a}{2kT} + T^{3/4}\left(\frac{-E_a}{2k}\right)\left(\frac{-1}{T^2}\right)\exp\frac{-E_a}{2kT}\right] \tag{C4}$$

$$\frac{dp}{dT} = \left(\frac{N_a 2}{g}\right)^{1/2} \left(\frac{2\pi m^* k}{h^3}\right)^{3/4} T^{3/4} \exp\frac{-E_a}{2kT}\left[\frac{3}{4T} + \frac{E_a}{2kT^2}\right] \tag{C5}$$

$$\frac{d\rho}{dT} = \rho\left[\frac{3}{4T} + \frac{E_g}{2kT^2}\right] \tag{C6}$$

Since:

$$\frac{\Delta\rho}{\rho} = \frac{d\rho}{dT}\,\frac{\Delta T}{\rho} \tag{C7}$$

then:

$$\frac{\Delta\rho}{\rho} = \left[\frac{3}{4T} + \frac{E_g}{2kT^2}\right]\Delta T \tag{C8}$$

or equivalently:

$$\frac{\Delta\rho}{\rho} = \left[\frac{3}{4} + \frac{E_g}{2kT}\right]\frac{\Delta T}{T} \tag{C9}$$

Vita

Gary E. Rattray was born on 10 April 1950 in Bath, New Brunswick, Canada. He graduated from high school in Easton, Maine in 1968 and attended the University of Maine from which he received the degree of Bachelor of Arts in Physics in May 1972. After receiving a commission in the USAF through the OTS program, he completed pilot training in April 1974. He then served as a flight training instructor at Webb AFB, Texas and Vance AFB, Oklahoma until entering the School of Engineering, Air Force Institute of Technology, in May 1978.

Permanent address: Route 2
Easton, Maine 04740

UNCLASSIFIED

SECURITY CLASSIFICATION OF THIS PAGE (When Data Entered)

REPORT DOCUMENTATION PAGE		READ INSTRUCTIONS BEFORE COMPLETING FORM
1. REPORT NUMBER AFIT/GEP/PH/79D-9	2. GOVT ACCESSION NO.	3. RECIPIENT'S CATALOG NUMBER
4. TITLE (and Subtitle) HIGH TEMPERATURE HALL EFFECT IN INDIUM-DOPED SILICON		5. TYPE OF REPORT & PERIOD COVERED MS Thesis 6. PERFORMING ORG. REPORT NUMBER
7. AUTHOR(s) Gary E. Rattray Captain		8. CONTRACT OR GRANT NUMBER(s)
9. PERFORMING ORGANIZATION NAME AND ADDRESS Air Force Institute of Technology (AFIT/EN) Wright-Patterson AFB, Ohio 45433		10. PROGRAM ELEMENT, PROJECT, TASK AREA & WORK UNIT NUMBERS
11. CONTROLLING OFFICE NAME AND ADDRESS Air Force Materials Laboratory (AFML-LPO) Wright-Patterson AFB, Ohio 45433		12. REPORT DATE December, 1979 13. NUMBER OF PAGES 82
14. MONITORING AGENCY NAME & ADDRESS(if different from Controlling Office)		15. SECURITY CLASS. (of this report) Unclassified 15a. DECLASSIFICATION/DOWNGRADING SCHEDULE

16. DISTRIBUTION STATEMENT (of this Report)

Approved for public release: distribution unlimited

17. DISTRIBUTION STATEMENT (of the abstract entered in Block 20, if different from Report)

18. SUPPLEMENTARY NOTES

Approved for public release; IAW AFR 190-17

JOSEPH M. HIPP, Major, USAF
Director of Public Affairs

19. KEY WORDS (Continue on reverse side if necessary and identify by block number)

Hall Effect
High Temperature Hall Effect
Indium-doped Silicon
Hall Scattering Factor
r-factor

20. ABSTRACT (Continue on reverse side if necessary and identify by block number)

Apparatus was designed and constructed to make resistivity and Hall coeffecient measurements at temperatures up to 875 degrees Kelvin. Data was taken on three indium-doped silicon samples, and resistivity, Hall mobility, and carrier concentration calculated for temperatures through the exhaustion region. The concentrations and activation energies of the various dopants were determined by fitting carrier concen-

DD FORM 1 JAN 73 1473 EDITION OF 1 NOV 65 IS OBSOLETE

UNCLASSIFIED

SECURITY CLASSIFICATION OF THIS PAGE (When Data Entered)